

## **Dark carbon fixation in the Arabian Sea oxygen minimum zone contributes to sedimentary organic carbon (SOM)**

LENGGER, Sabine K. <<http://orcid.org/0000-0003-4047-8773>>, RUSH, Darci <<http://orcid.org/0000-0002-6567-4116>>, MAYSER, Jan Peter, BLEWETT, Jerome, SCHWARTZ-NARBONNE, Rachel <<http://orcid.org/0000-0001-9639-9252>>, TALBOT, Helen M., MIDDELBURG, Jack J. <<http://orcid.org/0000-0003-3601-9072>>, JETTEN, Mike S.M. <<http://orcid.org/0000-0002-4691-7039>>, SCHOUTEN, Stefan, SINNINGHE DAMSTÉ, Jaap S. and PANCOST, Richard D.

Available from Sheffield Hallam University Research Archive (SHURA) at:

<http://shura.shu.ac.uk/25651/>

---

This document is the author deposited version. You are advised to consult the publisher's version if you wish to cite from it.

### **Published version**

LENGGER, Sabine K., RUSH, Darci, MAYSER, Jan Peter, BLEWETT, Jerome, SCHWARTZ-NARBONNE, Rachel, TALBOT, Helen M., MIDDELBURG, Jack J., JETTEN, Mike S.M., SCHOUTEN, Stefan, SINNINGHE DAMSTÉ, Jaap S. and PANCOST, Richard D. (2019). Dark carbon fixation in the Arabian Sea oxygen minimum zone contributes to sedimentary organic carbon (SOM). *Global Biogeochemical Cycles*.

---

### **Copyright and re-use policy**

See <http://shura.shu.ac.uk/information.html>

1 **Dark carbon fixation in the Arabian Sea oxygen minimum zone contributes to**  
2 **sedimentary organic carbon (SOM)**

3 **Sabine K. Lenger<sup>1,2,3\*</sup>, Darci Rush<sup>3</sup>, Jan Peter Mayser<sup>2</sup>, Jerome Blewett<sup>2</sup>, Rachel**  
4 **Schwartz-Narbonne<sup>4</sup>, Helen M. Talbot<sup>4,†</sup>, Jack J. Middelburg<sup>5</sup>, Mike S.M. Jetten<sup>6</sup>, Stefan**  
5 **Schouten<sup>3,5</sup>, Jaap S. Sinninghe Damste<sup>3,5</sup> and Richard D. Pancost<sup>2</sup>**

6 <sup>1</sup> Biogeochemistry Research Centre, School of Geography, Earth and Environmental Science,  
7 University of Plymouth, PL48AA, Plymouth, United Kingdom.

8 <sup>2</sup> Organic Geochemistry Unit, School of Chemistry, University of Bristol, BS81TS, Bristol,  
9 United Kingdom.

10 <sup>3</sup> NIOZ Royal Netherlands Institute for Sea Research, Dept. of Marine Microbiology and  
11 Biogeochemistry, and Utrecht University, 1797SZ, Texel, The Netherlands.

12 <sup>4</sup> School of Natural and Environmental Sciences, Newcastle University, Drummond Building,  
13 NE1 7RU, Newcastle-upon-Tyne, United Kingdom.

14 <sup>5</sup> Department of Earth Sciences, Faculty of Geosciences, Utrecht University, 3508 TA, Utrecht,  
15 The Netherlands.

16 <sup>6</sup> Department of Microbiology, IWWR, Radboud University Nijmegen, 6525 XZ, Nijmegen, The  
17 Netherlands

18 \* corresponding author: Sabine Lenger (sabine.lenger@plymouth.ac.uk)

19 † present address: BioArCh, Environment Building, University of York, YO10 5DD, Heslington,  
20 United Kingdom.

22 **Key Points:**

- 23 • One fifth of organic matter on Arabian Sea seafloor could stem from bacterial carbon  
24 fixation in the oxygen minimum zone
- 25 • Evaluation of past anoxic events needs to take chemoautotrophic contribution into  
26 account in isotope balances
- 27 • Biogeochemical models ignoring dark carbon fixation could highly underestimate oxygen  
28 demand and thus expansion of oxygen minimum zones

30 **Abstract**

31 In response to rising CO<sub>2</sub> concentrations and increasing global sea surface temperatures, oxygen  
32 minimum zones (OMZ), or “dead zones”, are expected to expand. OMZs are fueled by high  
33 primary productivity, resulting in enhanced biological oxygen demand at depth, subsequent  
34 oxygen depletion, and attenuation of remineralization. This results in the deposition of organic  
35 carbon-rich sediments. Carbon drawdown is estimated by biogeochemical models; however, a  
36 major process is ignored: carbon fixation in the mid- and lower water column. Here, we show  
37 that chemoautotrophic carbon fixation is important in the Arabian Sea OMZ; and manifests in a  
38 <sup>13</sup>C-depleted signature of sedimentary organic carbon. We determined the δ<sup>13</sup>C values of SOM  
39 deposited in close spatial proximity but over a steep bottom-water oxygen gradient, and the δ<sup>13</sup>C  
40 composition of biomarkers of chemoautotrophic bacteria capable of anaerobic ammonia  
41 oxidation (anammox). Isotope mixing models show that detritus from anammox bacteria or other  
42 chemoautotrophs likely forms a substantial part of the organic matter deposited within the  
43 Arabian Sea OMZ (~17%), implying that the contribution of chemoautotrophs to settling organic  
44 matter is exported to the sediment. This has implications for the evaluation of past, and future,  
45 OMZs: biogeochemical models that operate on the assumption that all sinking organic matter is  
46 photosynthetically derived, without new addition of carbon, could significantly underestimate the  
47 extent of remineralization. Oxygen demand in oxygen minimum zones could thus be higher than  
48 projections suggest, leading to a more intense expansion of OMZs than expected.

49 **Plain Language Summary**

50 Oxygen minimum zones are areas in the ocean in which algae produce large amounts of organic  
51 material. When this sinks towards the seafloor, all oxygen at depth is used up. This results in vast  
52 “dead zones” where almost no oxygen is available to sustain life. With global warming, and  
53 increased nutrients from rivers, dead zones are forecast to expand. Computer models can  
54 calculate this, by considering algal production, and the amount of material delivered to the  
55 seafloor. However, these models often ignore a major process: anaerobic bacteria in the deeper  
56 water column, that can live at the edge or in the middle of these dead zones, which can also  
57 produce organic material from the dissolved CO<sub>2</sub>. In this study, we used the fact that these  
58 bacteria add a distinct signature to the organic material, to show that one fifth of the organic  
59 matter on the seafloor could stem from bacteria living in these dead zones. Thus, models that  
60 have missed out on considering this contribution could have underestimated the extent of oxygen  
61 depletion we are to expect in a future, warming world. A more intense expansion of dead zones  
62 than expected could have severe ecological, economical (fisheries), and climatic consequences.

63

64     **1 Introduction**

65     Marine primary production fixes 50 Pg carbon per year, of which only about 1% is buried  
66     in sediments (Dunne et al., 2007; Middelburg, 2011). The majority of organic carbon derived  
67     from the photic zone is remineralised during sedimentation, fueling heterotrophic bacterial  
68     activity in the water column (Keil et al., 2016). In marginal settings and OMZs, marine primary  
69     production in the photic zone can be significantly higher than in other settings. Organic carbon  
70     (OC) sedimentary accumulation rates within an OMZ can be in the range of tens to hundreds of  
71     mg C cm<sup>-2</sup> y<sup>-1</sup> (Hartnett et al., 1998; Hedges and Keil, 1995) higher than observed in other parts  
72     of the ocean. These high accumulation rates are most commonly attributed to attenuation in  
73     remineralization rates within the OMZ, and low bottom-water oxygenation, which results in  
74     decreased biodegradability of polymeric and matrix-protected substances (Burdige, 2007).

75     As a consequence of increasing atmospheric CO<sub>2</sub> concentrations and, consequently,  
76     temperature, oceanic OMZs are forecast to expand in a fashion similar to the past (Breitburg et  
77     al., 2018; Queste et al., 2018; Schmidtko et al., 2017; Shaffer et al., 2009; Stramma et al., 2010).  
78     Whilst the expansion of OMZs will result in widespread habitat loss of marine life and could  
79     cause an increase in emissions of greenhouse gases such as N<sub>2</sub>O and CH<sub>4</sub>, it could also act as a  
80     long-term negative feedback on global warming via the enhanced drawdown and storage of  
81     organic carbon in sediments.

82     The biogeochemical system in subsurface waters, where light does not penetrate, has  
83     recently emerged to be substantially more complex – and possibly more important for the global  
84     carbon cycle – than previously assumed. In particular, dark water-column microbial activity is  
85     higher than what can be accounted for by heterotrophs (Herndl and Reinhäler, 2013), suggesting  
86     an important role for chemoautotrophy, i.e. fixation of dissolved inorganic carbon (DIC). It has  
87     been suggested to contribute substantially to the global carbon budget, with estimates ranging  
88     from 0.11 to 1.1 Pg C y<sup>-1</sup>, equating to ca. 2% of total estimated yearly marine primary production  
89     (Middelburg, 2011; Reinhäler et al., 2010). The predominant chemoautotrophic process in the  
90     oxic, dark, pelagic ocean is thought to be nitrification (Middelburg, 2011; Pachiadaki et al.,  
91     2017). When oxygen is limited, nitrification still occurs, but other chemoautotrophic processes  
92     dominate, such as anaerobic oxidation of ammonia and sulfide oxidation (Ulloa et al., 2012;  
93     Wright et al., 2012).

94     Under hypoxic conditions, such as in the water column of OMZs, both archaeal (aerobic)  
95     and anaerobic oxidation of ammonia are thought to dominate dark inorganic carbon fixation  
96     processes (Lam and Kuypers, 2010; Pitcher et al., 2011). Here, nitrite accumulates, and other  
97     anaerobic autotrophic processes such as sulfide oxidation and methanogenesis are suppressed,  
98     most likely due to the abundance of nitrate and ammonia (Canfield, 2006; Ulloa et al., 2012).

99     Of the inorganic carbon converted to organic matter within the OMZ, only a negligible  
100    fraction is presumably transported to the sediments and preserved, as this newly produced  
101    material is regarded as more labile than the sinking OC derived from the photic zone (Cowie and  
102    Hedges, 1992; Keil et al., 1994; Middelburg, 1989). Dark carbon fixation rates are challenging to  
103    quantify: they have been determined experimentally (Reinhäler et al., 2010; Taylor et al., 2001),  
104    or have been estimated from the reaction stoichiometry of respiration based on Redfield organic  
105    matter and growth yields of nitrifiers (Middelburg, 2011; Wuchter et al., 2006). In OMZs, such  
106    as the Peruvian margin (Lam et al., 2009), the Arabian Sea (Jensen et al., 2011), or the sulfidic  
107    Black Sea (Lam et al., 2007), the activity of some chemoautotrophs was determined via <sup>15</sup>N-

108 labelling, and formation of the products of their biogeochemical reactions. However, incubation  
109 methods may suffer from bias, because *in situ* conditions such as pressure are difficult to  
110 maintain.

111 However, carbon from within anoxic waters has been observed in some settings to  
112 contribute to the particulate OC flux: for example, in eutrophic lakes (Hollander and Smith,  
113 2001) and anoxic fjords (van Breugel et al., 2005b). Furthermore, discrepancies between  
114 modelled and observed organic carbon fluxes suggest that dark carbon fixation in anoxic marine  
115 settings significantly contributes to sinking material (Keil et al., 2016; Taylor et al., 2001).

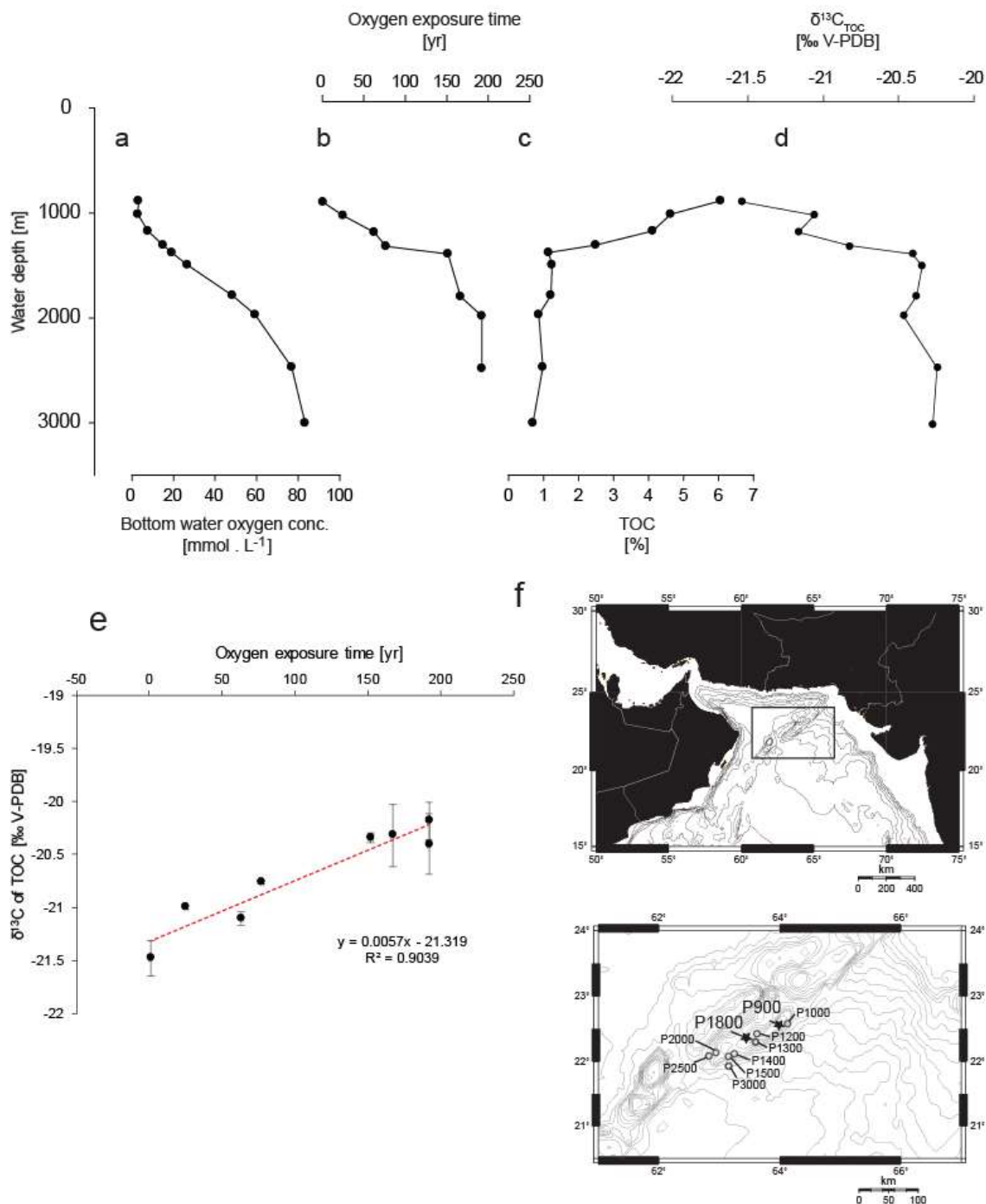
116 One way to constrain this input into sedimentary organic matter is to use isotope mixing  
117 models. Photosynthetically fixed carbon generally has stable carbon isotopic compositions of ca  
118 -19 to -21 ‰ due to Rubisco fixation. However, chemoautotrophs dwelling in OMZs typically  
119 have a lower  $\delta^{13}\text{C}$  values. This is the result of multiple factors: they either use  $^{13}\text{C}$ -depleted  $\text{CO}_2$   
120 generated by remineralization, have larger fractionation factors due to the higher abundance of  
121  $\text{CO}_2$  at depth (Freeman et al., 1994), or use carbon fixation pathways such as the acetyl  
122 coenzyme A pathway, which results in  $^{13}\text{C}$ -depleted biomass (Hayes, 2001). This characteristic  
123 chemoautotrophic isotopic signature in the organic carbon could allow us to quantify the  
124 contribution of dark carbon fixation to sedimentary organic matter.

125 Here, we investigated the  $\delta^{13}\text{C}$  value of sedimentary organic matter of surface sediments  
126 deposited within the OMZ of the Arabian Sea and employed a simple isotope mixing model to  
127 investigate the extent of input from OMZ carbon fixation into sedimentary organic matter. As the  
128 major process in the Arabian Sea OMZ known to produce isotopically light biomass is anaerobic  
129 oxidation of ammonia (anammox; Ulloa et al., 2012; Villanueva et al., 2014), in order to  
130 determine the isotopic signature of this pathway, we developed and applied a method to  
131 determine the  $\delta^{13}\text{C}$  values of a novel biomarker, bacteriohopanetetrol stereoisomer (BHT'),  
132 which has been found to be unique to anammox bacteria in the marine environment in culture  
133 and environmental studies (Rush et al., 2014, 2019; Rush and Sinninghe Damsté, 2017). It has  
134 been found in the Arabian Sea and other marine anoxic settings (Matys et al., 2017; Sáenz et al.,  
135 2011). We also used stable isotope probing experiments to exclude sedimentary anammox as an  
136 important contributor to this process. This allowed us to investigate the contribution of these  
137 dark carbon fixers to sedimentary organic carbon.

## 138 2 Materials and Methods

### 139 2.1 Sediment sampling and stable isotope probing incubations

140 Sediments were collected with multicore devices on the R/V Pelagia in the Northern  
141 Arabian Sea in January 2009 during the PASOM cruise 64PE301 along the Murray Ridge (Fig.  
142 1f), which protrudes into the core of the OMZ. Two cores, one each from P900 (885 m water  
143 depth) and P1800 (1786 m water depth), hereinafter referred to as anoxic and oxic, respectively,  
144 were incubated on board as described by Pozzato et al. (2013 a, b). In brief, particulate or  
145 dissolved organic matter from the diatom *Thalassiosira pseudonana* containing 20 and 18 %  $^{13}\text{C}$ ,  
146 respectively, were added to the tops of core tubes of 10 cm internal diameter. Between 2 and 6 %  
147 of the added carbon was respired, resulting in a highly enriched  $^{13}\text{C}_{\text{DIC}}$  pool, enabling the tracing  
148 of autotrophic processes in addition to heterotrophic processes.



150  
151  
152 **Figure 1.** Arabian Sea depth gradients. Shown are  $\delta^{13}\text{C}_{\text{org}}$  and % TOC values of core top  
153 sediments, and bottom water oxygenation plotted with depth (a-d), all but  $\delta^{13}\text{C}_{\text{org}}$  replotted from  
154 Lengger et al. (2014), a scatter plot of oxygen exposure time versus  $\delta^{13}\text{C}_{\text{org}}$  in Arabian Sea core  
155 tops along Murray Ridge (e), and a map of the sampling stations with the two main stations used  
156 for BHT analysis used here indicated with a star (f).

157        Eight cores are discussed here; these were incubated under oxic or suboxic conditions for  
158      7 days (125 µM, 6 µM O<sub>2</sub>, respectively; Table 1). At the end of incubation, cores were sliced in  
159      the intervals 0 – 2, 2 – 4, and 4 – 10 cm depth. They were then frozen and freeze dried for the  
160      isotopic analysis of the bacteriohopanepolyol lipids (BHPs), including bacteriohopanetetrol  
161      (BHT) and its stereoisomer and biomarker for anammox bacteria, BHT'. Both biomarkers have  
162      been studied previously in the Arabian Sea water column and sediments (Jaeschke et al., 2009;  
163      Sáenz et al., 2011) Furthermore, cores from 8 stations between 900 and 3000 m water depth were  
164      also collected, as described by Lengger et al. (2014, 2012b). The top 0 – 0.5 cm were used for  
165      total organic carbon (TOC) and <sup>13</sup>C of organic carbon analysis. For the core from P900 (32 cm  
166      length), all depths were analysed in 0.5 cm – 4 cm resolution (Lengger et al., 2012b).

167      2.2     Anammox enrichment cultures

168        To determine the δ<sup>13</sup>C values for the two bacteriohopanetetrols in anammox bacteria  
169      (BHT and BHT', the latter being unique to anammox in the marine environment), an enrichment  
170      culture of '*Ca. Scalindua profunda*' was analysed. It was grown in a sequencing batch reactor as  
171      described by van de Vossenberg et al. (2008). Analysis of this enrichment culture that showed  
172      '*Ca. S. profunda*' comprised about 80% of the cells, while other bacteria belonging to the phyla  
173      Bacteriodetes (including Flavobacteriaceae) and Proteobacteria (including Alphaproteobacteria)  
174      accounted for the majority of the remaining populations (van de Vossenberg et al., 2008, 2013).

175      2.3. Extraction and purification

176        The freeze-dried subsamples of the unamended and incubated cores were ground, and the  
177      homogenised sediments and the culture were extracted by a modified Bligh-Dyer extraction  
178      method (Lengger et al., 2012a). Briefly, they were extracted ultrasonically three times in a  
179      mixture of methanol/dichloromethane (DCM)/phosphate buffer (2:1:0.8, v:v:v) and centrifuged,  
180      and the solvent phases were combined. The solvent ratio was then adjusted to 1:1:0.9, v:v:v to  
181      separate the DCM phase. Liquid extraction was repeated two more times, the DCM fractions  
182      were combined, the solvent was evaporated and the larger particles were filtered out over glass  
183      wool. The extraction procedure was performed on the enrichment culture material and repeated  
184      on the sediment for analysis of BHPs. An aliquot of the extract was subjected to column  
185      chromatography using 5% aminopropyl solid phase extraction (SPE), eluting with hexane, DCM,  
186      and MeOH, which contained BHPs. For analysis by chromatographic techniques, the extract was  
187      derivatised in 0.5 mL of a 1:1 (v:v) mixture of acetic anhydride and pyridine at 50 °C for 1 h,  
188      then at room temperature overnight in the case of HPLC-MS analysis. Solvent was dried under a  
189      stream of N<sub>2</sub> on a 50°C heating block.

190      2.4. Instrumental techniques

191      2.4.1. High temperature gas chromatography coupled to flame ionization detection (HTGC-FID)

192        GC analysis of acetylated BHPs was done using a HP-5890 Series II GC equipped with a  
193      flame ionization detector was fitted with a 0.25 mm x 0.1 µm VF5-ht capillary column (CP9045,  
194      CP9046, Agilent Technologies UK Ltd., Stockport, UK) of 30 m length (Lengger et al., 2018).  
195      An on-column injector was used. To the 30 m column, 1m of a 0.25 mm HT-deactivated silica  
196      tubing was attached as a guard column (Zebtron Z-Guard, 7CG-G000-00GH0, Phenomenex,  
197      Macclesfield, UK). Analysis of bacteriohopanepolyols employed a constant flow of 2 ml/min He  
198      and a temperature ramp from 70°C (1 min hold) to 400°C at 7°C min<sup>-1</sup> (1 min hold).

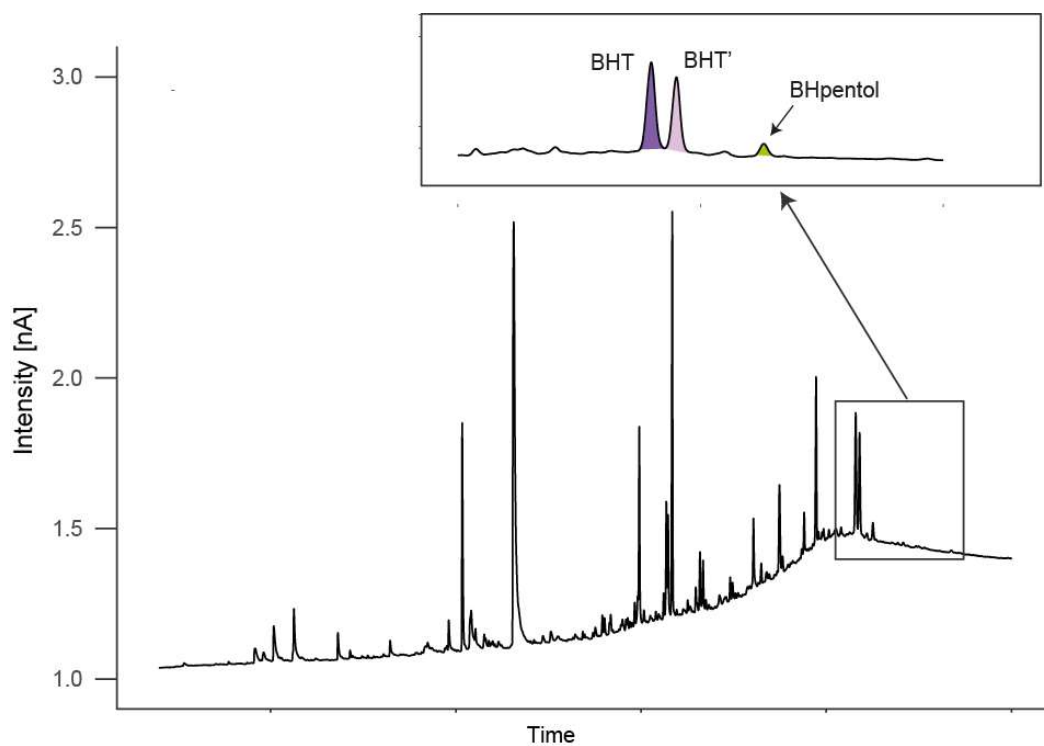
199 2.4.2. High temperature gas chromatography coupled to mass spectrometric detection (HTGC-  
200 MS)

201 Analysis of acetylated BHPs, using HTGC-MS was performed using a Thermo Scientific  
202 Trace 1300 gas chromatograph coupled with an ISQ single quadrupole mass spectrometer.  
203 Diluted samples were introduced using a PTV injector in splitless mode onto a 0.53 mm fused  
204 silica pre-column connected to a 30 m × 0.25 mm i.d. fused-silica capillary column coated with  
205 dimethyl polysiloxane stationary phase (ZB-5HT; film thickness, 0.1 µm; 7HG-G015-02,  
206 Phenomenex, Macclesfield, UK). The initial injection port temperature was 70 °C with an  
207 evaporation phase of 0.05 min, followed by a transfer phase from 70 °C to 400 °C at 0.2 °C s<sup>-1</sup>.  
208 The oven temperature was held isothermally for 1 min at 70 °C, increased at a rate of 7 °C min<sup>-1</sup>  
209 to 400 °C and held at 400 °C for 10 min. Helium was used as a carrier gas and maintained at a  
210 constant flow of 2.5 ml min<sup>-1</sup>. The mass spectrometer was operated in the electron ionization  
211 (EI) mode (70 eV) with a GC interface temperature of 400 °C and a source temperature of  
212 340 °C. The emission current was 50 µA and the mass spectrometry set to acquire in the range of  
213 *m/z* 50–950 Daltons with 0.5 s dwell time. Data acquisition and processing were carried out  
214 using the Thermo XCalibur software (version 3.0.63). Due to the lack of authentic standards for  
215 BHT and BHT', only relative and not absolute values are reported, assuming similar ionization  
216 energies.

217 2.4.3. High temperature gas chromatography coupled to isotope ratio mass spectrometry (HTGC-  
218 IRMS)

219 The stable carbon isotopic composition ( $\delta^{13}\text{C}$ ) of BHPs were determined using HTGC-  
220 isotope ratio mass spectrometry. To this end, an Elementar visION IRMS with GC5 interface  
221 (Elementar UK Ltd., Cheadle, UK), and an Agilent 7890B GC were modified in-house and  
222 allowed us to achieve column temperatures of up to 400 °C, which resulted in baseline resolution  
223 of BHT and BHT' (Fig. 2). 1 µl of the derivatized samples dissolved in ethyl acetate were  
224 injected on a cool-on-column injector, into a Zebron Z-Guard Hi-Temp Guard Column (1 m x  
225 0.25 mm, Zebron Z-Guard, 7CG-G000-00GH0, Phenomenex, Macclesfield, UK) and separated  
226 on a Zebron ZB-5HT analytical column (30 m x 0.25 mm x 0.1 µm, Phenomenex Ltd.,  
227 Macclesfield, UK). He was used as a carrier gas at a flow rate of 1.5 ml min<sup>-1</sup> and the oven was  
228 programmed as follows: 1 min hold at 70 °C, increase by 7 °C min<sup>-1</sup> to 350 °C (10 min hold).  
229 Organic compounds were combusted to CO<sub>2</sub> in a 0.7 mm ID quartz tube with CuO pellets at  
230 850°C. Instrumentation performance was monitored using an n-alkane standard (B3, A.  
231 Schimmelmann, Indiana University, Bloomington, IN, USA; RMS 0.4 %), and results were  
232 calibrated using an in-house mixture of five fatty acid methyl esters, which was injected between  
233 every six sample analyses and analyzed using a He flow of 1 ml min<sup>-1</sup>, with a slightly different  
234 temperature program (injection at 50 °C held for 1 min followed by an increase of 10°C min<sup>-1</sup> to  
235 300 °C and a 10 min hold). This is the first time baseline resolution between BHT and BHT' has  
236 been achieved on a GC-IRMS, which allows the direct determination of the isotopic composition  
237 of both BHT and BHT' in sediment samples (Fig. 2). The isotopic composition of the acetyl  
238 group used to derivatise the BHT and BHT' was determined by acetylation of *myo*-inositol, and  
239 then subtracted from the values of BHT and BHT' in a mass balance correction (Angelis et al.,  
240 2012), as authentic standards for BHT or BHT' were not available.

241



242  
243 **Figure 2.** HTGC-IRMS chromatogram showing baseline separation between BHT, BHT', and  
244 BHpentol.

245 2.4.4. High performance liquid chromatography coupled to positive ion atmospheric pressure  
246 chemical ionization mass spectrometry (HPLC/APCI-MS)

247 To verify the GC-derived assignments, an aliquot of the acetylated BHP samples was  
248 dissolved in MeOH:propan-2-ol (3:2; v:v) and filtered on 0.2 µm PTFE filters. BHPs were  
249 analysed by HPLC/APCI-MS, using a data-dependent scan mode (3 events) on an HPLC system  
250 equipped with an ion trap MS, as described in Talbot et al. (2007) and van Winden et al. (2012).  
251 Relative BHP concentrations were semi-quantitatively estimated based on the response factor of  
252 authentic standards (M. Rohmer; Strasbourg, France; Cooke et al., 2008), with a typical  
253 reproducibility of ± 20%, according to Cooke et al. (2009).

254 2.4.5. Bulk sedimentary organic matter and suspended particulate matter

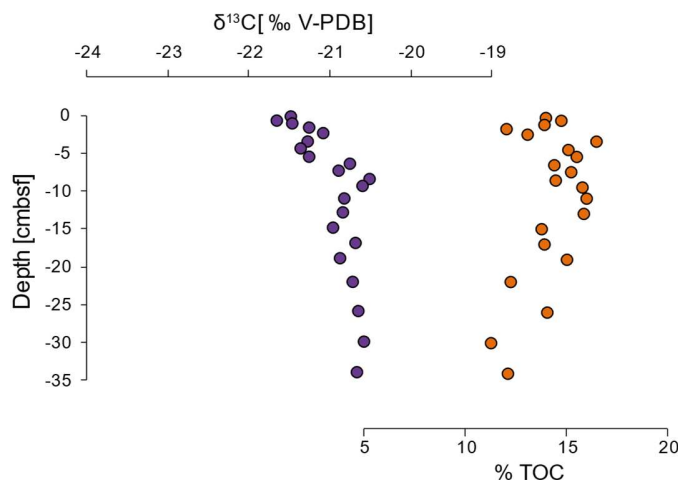
255 Freeze-dried core tops from 8 stations between 900 and 3000 m for sedimentary organic  
256 matter, and punches from 0.7 µm GFF filters for suspended particulate organic matter, were  
257 decalcified with 2N HCl, washed, freeze-dried, and subjected to analysis via a Flash EA 1112  
258 Series (Thermo Scientific) analyser, coupled via a Conflo II interface to a Finnigan Delta<sup>plus</sup>  
259 mass spectrometer as described by Lengger et al. (2014; sediment) and Pitcher et al. (2011;  
260 filters). Standards for δ<sup>13</sup>C analysis were acetanilide and benzoic acid and samples were analysed  
261 in duplicate.

262     **3. Results**

263     To quantify the provenance of sedimentary organic matter and the contribution of  
264     anammox from the OMZ, we analysed the isotopic composition of sedimentary organic matter  
265     deposited in close spatial proximity over a large depth gradient in the Arabian Sea, as well as the  
266     isotopic composition of biomarker lipids derived from anammox bacteria, chemoautotrophic  
267     microbes living in the OMZ. In order to determine whether these were water-column derived or  
268     sedimentary, we used stable isotope probing experiments on sediments retrieved from within and  
269     below the OMZ.

270     **3.1.  $\delta^{13}\text{C}$  values of  $\text{C}_{\text{org}}$**

271  
272      $\delta^{13}\text{C}$  values of  $\text{C}_{\text{org}}$  in surface sediments were low (-21.5 ‰) at P900 and increased with  
273     water depth to -20.2 ‰ at P2500 (Fig. 1d).  $\delta^{13}\text{C}_{\text{org}}$  values correlated positively and linearly  
274     (Slope 0.0057,  $R^2 = 0.90$ , Figure 1e) with oxygen exposure times as calculated by Koho et al.  
275     (2013) and Lengger et al. (2014). Similarly, organic carbon content in the core tops was  
276     negatively correlated with oxygen exposure times ( $R^2 = 0.93$ , from Lengger et al., 2014). The  
277     increase mirrors the decrease in % TOC – and thus progressing degradation – with increasing  
278     oxygen exposure time (Fig. 1b,c, Lengger et al., 2014). At P900, where the whole depth of the  
279     core was analysed, values increased slightly with depth, from -21.5 ‰ at the surface, to -20.9 ‰  
280     (Fig. 3).  $\delta^{13}\text{C}$  values of particulate organic carbon (suspended particulate organic matter)  
281     decreased throughout the water column from -19 to -21.8 ‰, though with a substantially  $^{13}\text{C}$ -  
282     depleted, yet unexplained, value at the very surface (20 m depth) of -22.9 ‰ (Fig. S1).



284  
285     **Figure 3.** Depth profile of  $\delta^{13}\text{C}_{\text{org}}$  and % TOC in an unamended core at P900.

286     **3.2. Biomarkers**

287         **3.2.1. Bacteriohopanepolyols (BHPs)**

288  
289     Analysis of BHPs in the Arabian Sea cores using both HPLC-APCI-MS and HTGC-MS,  
290     all showed that BHT', specific for *Scalindua*, was abundant, and the fractional abundance of  
291     BHT's when compared to the sum of BHT and BHT' ranged from 0.4 to 0.6. Other, relatively  
292     non-source-specific, BHPs were also present: BHT, 35-aminobacteriohopane-32,33,34-triol

(aminotriol), bacteriohopane-31,32,33,34,35-pentol (BHpentol), bacteriohopanetetrol cyclitol ether (BHT-CE) and anhydro-BHT (Fig. S3). The relative concentrations of bacteriohopanetetrols were 75 to 96 % of total bacteriohopanepolyols, an order of magnitude higher than other BHPs (Fig. S3). HTGC-MS was able to detect BHT, BHT' and BHpentol (Fig. S2), as well as small amounts of anhydroBHT, a BHT degradation product, and BHP-570, which has been tentatively identified by Sessions et al. (2013) as acetylated bacteriohopanediol, possibly also a degradation product of bacteriohopanetetrol. In the core from P900, the ratio of BHT' over BHT increased with depth (Fig. S4).

We also analysed the BHP content of sediment cores incubated with  $^{13}\text{C}$ -labelled organic matter at both sites under the different conditions detailed by Pozzato et al. (2013 a, b), which was respired and generated  $^{13}\text{C}$ -labelled DIC, allowing to trace autotrophic processes such as anammox. No changes were noted, except for in P900; in those, BHT abundance increased (i.e. BHT'/BHT decreased), indicating that some of the sedimentary BHT could have been produced in situ (Fig. S4).

### 3.2.2. BHT and BHT' $\delta^{13}\text{C}$ values

To establish the isotopic difference of BHT and BHT' derived from anammox we analysed biomass obtained from a batch reactor. BHT and BHT' were the main biohopanoids in the biomass from '*Ca. S. profunda*' detected by HTGC-MS (Fig. S2b). In addition to being present in '*Ca Scalindua* sp.' anammox bacteria, BHT is a ubiquitous lipid common to many bacteria, BHT', however, is specific to '*Ca Scalindua* sp.' in marine environments (Rush et al., 2014). The  $\delta^{13}\text{C}$  values of BHT and BHT' were identical within the error of analysis (-49 and -48 ‰, respectively; Table 1), indicating identical fractionation and thus biosynthetic pathways for both lipids.

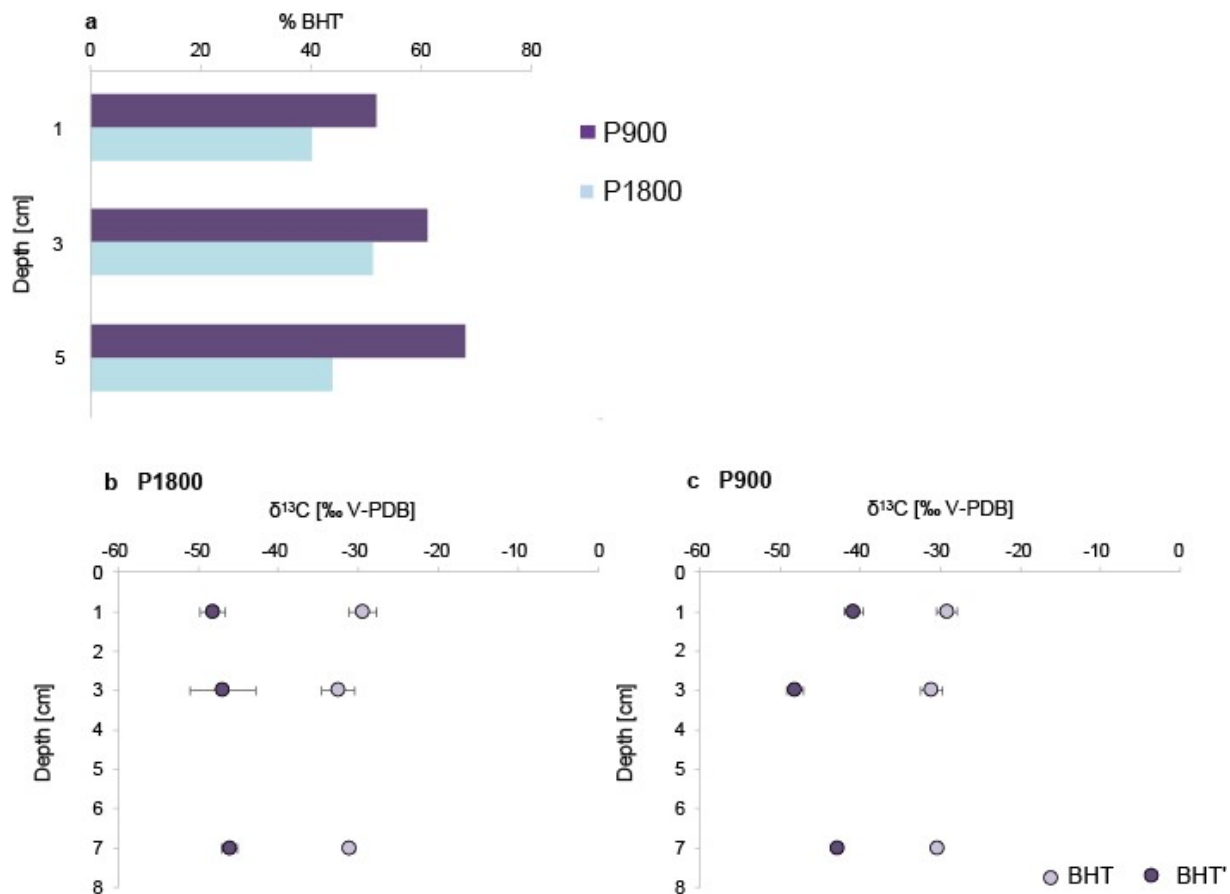
In the Arabian Sea sediments (all unamended cores), BHT was markedly enriched in  $^{13}\text{C}$  relative to BHT', with values ranging from -24.7 to -28.8 ‰ and -39.1 to -48.1 ‰, respectively (Figs. 4b-c). At P1800 (below the OMZ), BHT and BHT' were slightly more depleted in  $^{13}\text{C}$ , with BHT at  $-27 \pm 3$  ‰ and BHT' at  $-47 \pm 4$  ‰, as compared to  $-26 \pm 1$  ‰ and  $-43 \pm 5$  ‰ for BHT and BHT' at P900 (in the OMZ). However, the difference between P900 and P1800 was not statistically significant for either BHT or BHT'. Moreover, even though the proportion of BHT' increased with depth in the anoxic core, the  $\delta^{13}\text{C}$  values did not change. We also analysed BHT and BHT' in the cores that had been incubated with  $^{13}\text{C}$ -labeled POM and DOM, and these showed no indication of  $^{13}\text{C}$ -enrichment in BHT'. Excluding outliers (defined by a Grubbs test at 99% confidence level and indicated in Table 1), BHT' values were on average  $-48 \pm 4$  ‰ and  $-46 \pm 2$  ‰ at P1800, and P900, respectively. BHT was slightly enriched compared to the unamended incubations at 3 cm depth ( $\Delta\delta^{13}\text{C} = 4.6 \pm 0.7$  ‰), but not at 1 cm depth. BHpentol concentrations were too low to allow reliable isotopic determination, and anhydroBHT and BHP-570 co-eluted with other compounds, also precluding their isotopic characterization.

## 4. Discussion

### 4.1. Origins of BHT and BHT' - a biomarker for anammox

BHT', a biomarker likely unique for anammox in marine environments (Rush et al., 2014,), is highly abundant in the sediment and occurred throughout both sediment cores (Fig. 4a), suggesting a significant contribution of anammox biomass to sedimentary organic matter. In

336 the anoxic core (P900), BHT and BHT' were present in concentrations at least an order of  
 337 magnitude higher than other BHPs (Fig. S2), and BHT' was the most abundant of the two  
 338 stereoisomers (Fig. 4a). The high fractional abundance of BHT' over the sum of BHT and BHT'  
 339 (0.4 – 0.6) is contrary to our expectations, as BHT is a ubiquitous lipid and presumed to derive  
 340 from both anammox and non-anammox sources such as cyano- and many other bacteria (Pearson  
 341 and Rusch, 2009); it is, therefore, expected to be abundant in most depositional contexts. Lower  
 342 proportions of BHT were reported previously in nearby core tops (0.22-0.30) by Saenz et al.  
 343 (2011); this could be caused by a difference in settings, or in BHP extraction protocol. However,  
 344 the high proportions of BHT' observed in the Arabian Sea are not unprecedented: they are  
 345 slightly lower than BHT' proportions in sediments underlying the Humboldt Current System  
 346 OMZ offshore Peru (0.45 – 0.69 in surface sediments, Matys et al., 2017).



347  
 348  
 349 **Figure 4.** Anammox biomarkers in unamended Arabian Sea sediment. Panel (a) shows the  
 350 proportion of BHT' relative to BHT+BHT', panels (b) and (c) show the  $\delta^{13}\text{C}$  values of BHT and  
 351 BHT' in the unamended oxic (P1800) and anoxic core (P900), respectively.  
 352

353 Supporting evidence for the unique source of BHT' comes from its  $^{13}\text{C}$  values of -40 to -  
 354 50‰. Anammox bacteria are known to fractionate strongly against  $\delta^{13}\text{C}$ , with up to 26 ‰  
 355 fractionation observed for biomass in cultures and sediment, with even more strongly depleted  
 356 BHT and BHT' (Brocadia sp. by 47 ‰ and Scalindua sp. by 49 ‰ against DIC; Schouten et al.,  
 357 2004). Anammox bacteria within the oxygen minimum zone and using dissolved inorganic

358 carbon, which is up to 2 ‰ lighter within the OMZ than at the surface (Kroopnick, 1984), are  
359 likely to produce such  $^{13}\text{C}$ -depleted lipids. In line with an anammox origin, BHT' here is  
360 decidedly more depleted than other biomarkers in the Arabian Sea (cf. Wakeham and McNichol,  
361 2014), though distinctly depleted highly branched isoprenoids (HBIs, -37 ‰) have been found in  
362 Arabian Sea cores from the Holocene (Schouten et al., 2000).

363 BHT, however, is much more enriched in  $^{13}\text{C}$  in the Arabian Sea sediments, with values  
364 of -29 to -30 ‰ (Fig. 4b,c). This is in contrast to anammox cultures, where BHT and BHT' are  
365 produced with identical isotope values (Fig. S4, Table 1). This strongly supports the idea that  
366 BHT has a mixed origin. The sources for BHT could be varied: cyanobacteria or heterotrophic  
367 bacteria thriving in the OMZ or the sediment (Pearson and Rusch, 2009), and possibly including  
368 nitrite-oxidising bacteria (Kharbush et al., 2018). The  $\delta^{13}\text{C}$  values of BHT derived from these  
369 alternative sources are poorly constrained (Hayes, 2001; Kharbush et al., 2018; Pearson, 2010;  
370 Sakata et al., 1997; Schouten et al., 1998). However, for heterotrophic bacteria, values similar to  
371 the consumed OM minus the depletion associated with polyisoprenoids of 6–8 ‰ are expected  
372 (Pancost and Sinninghe Damsté, 2003). Similar values would be expected for cyanobacterial  
373 lipids, too, as those are depleted by 22–30 ‰ compared to dissolved  $\text{CO}_2$ , which varies from 0  
374 to 2 ‰ in the photic zone. Methane cycling could also lead to  $^{13}\text{C}$  depleted OM, but is not  
375 important in the Arabian Sea (Lüke et al., 2016), and there is no biomarker evidence for it, such  
376 as  $^{13}\text{C}$  depleted archaeal lipids, or methylated BHPs. Thus, a BHT  $\delta^{13}\text{C}$  value of -30 ‰ suggests  
377 heterotrophic and other bacterial sources, possibly mixed with an anammox source.

378 Anammox activity has been shown to occur both within the OMZ water column (Jensen  
379 et al., 2011; Lüke et al., 2016; Pitcher et al., 2011; Villanueva et al., 2014) as well as in  
380 sediments (Sokoll et al., 2012; Devol, 2015). To test whether the anammox-derived biomarkers  
381 are formed in the sediment, the labelled cores were incubated for 7 days with particulate and  
382 dissolved organic matter (Table 1), which resulted in the substantial incorporation of  $^{13}\text{C}$  into  
383 bacterial fatty acids, as well as generating  $^{13}\text{C}$ -enriched  $\text{CO}_2$  due to heterotrophic respiration (up  
384 to 14 % of the added C was respired, Pozzato et al., 2013a,b). Anammox bacteria are  
385 autotrophic, and it is therefore likely that an active sedimentary community would result in some  
386 uptake of this  $^{13}\text{C}$  labelled  $\text{CO}_2$  formed by respiration. However, no significant labelling was  
387 observed in BHT' or BHT (Table 1, Table S1), suggesting that most of this pool is water-column  
388 derived. Further, BHT and BHT' are also present in the surface of the oxic sediments (P1800), in  
389 proportions similar to the anoxic sediments at P900. Even if anammox growth was too slow for  
390 labelling to take effect, substantial sedimentary production would have resulted in a decreasing  
391  $\delta^{13}\text{C}$  value of BHT' in the unamended cores, as DIC gradually becomes more  $^{13}\text{C}$  depleted with  
392 sediment depth (Fernandes et al., 2018), but this is not observed (Fig. 4bc). Collectively, these  
393 data support the idea that the vast majority of BHT' is derived from anammox bacteria living in  
394 the OMZ of the water column, and that BHT also has a predominant pelagic origin with limited  
395 sedimentary production.

396 The  $\delta^{13}\text{C}$  values of geohopanoids (i.e. the geological degradation product of biohopanoids such  
397 as BHT and BHT') can exhibit dramatic variability, and often pronounced depletion in terrestrial  
398 (Pancost et al., 2007) and marine settings (Köster et al., 1998). These are commonly attributed to  
399 aerobic methane oxidising bacteria, and thus regarded as evidence for a significant contribution  
400 of methane oxidisers to sedimentary organic matter. However, our data show that hopanes of -35  
401 to -50 ‰ could also indicate the presence of a significant amount of anammox bacteria in an  
402 anoxic water column. Several factors could attenuate the anammox signal. The decrease of

403 biohopanoids in structural complexity upon degradation means that the anammox signal would  
404 be diluted by mixing with aerobically and anaerobically produced hopanoids such as those of  
405 *Geobacter* (Fischer et al., 2005; Härtner et al., 2005). Chemoautotrophs operating in euxinic  
406 settings employ biochemical pathways resulting in  $^{13}\text{C}$ -enriched biomass and lipids compared to  
407 DIC (van Breugel et al., 2005b). However, in anoxic basins such as the Black Sea or anoxic  
408 fjords, remineralization of organic matter also results in distinctly depleted  $\delta^{13}\text{C}_{\text{DIC}}$  below the  
409 chemocline (-12 ‰; Fry et al., 1991; Volkov, 2000). This may explain why, in some marine  
410 anoxic settings where we might expect to see an anammox signature, the  $^{13}\text{C}$  depletion of  
411 hopanes parallels that of algal biomarkers (Sinninghe Damsté et al., 2008; van Breugel et al.,  
412 2005a). Nonetheless, we suggest that potential anammox contributions to the sedimentary  
413 hopanoid pool should be considered when interpreting their abundances, distributions and  
414 isotopic compositions.

415 4.2. Origin of sedimentary organic matter

416 The Murray Ridge represents an open ocean setting, and the selected coring sites were in  
417 close proximity to each other, with no substantial terrigenous contribution (Koho et al., 2013;  
418 Lenger et al., 2014, 2012b; Nierop et al., 2017; Fig. 1d). Despite this,  $\delta^{13}\text{C}$  values of  
419 sedimentary organic matter of a purely marine origin varied: The value at the shallowest location  
420 (-21.5 ‰; P900), within the OMZ, was 2.5 ‰ more depleted than the estimated value for surface  
421 water-derived OM -19.8 ‰ (Fontugne and Duplessy, 1986), and the  $\delta^{13}\text{C}$  values of sedimentary  
422  $\text{C}_{\text{org}}$  increased with increasing oxygen bottom water concentrations / oxygen exposure time (Fig.  
423 1e). These observations agree with earlier studies from this setting. Cowie et al. (2009, 1999)  
424 detected similar trends in surficial sediments across different settings in the Arabian Sea, with  
425 values of -21 ‰ within and -19 ‰ above and below the OMZ. Organic matter in sediment traps  
426 collected in the north western Arabian Sea (i.e. sinking POC) had a  $\delta^{13}\text{C}$  value of -22.4 ‰  
427 (composite of the OMZ between 500 and 900 m depth). The corresponding sedimentary  $\delta^{13}\text{C}_{\text{org}}$   
428 value, from oxygenated bottom waters at 1445 m depth, was, however, more enriched (-20.8‰;  
429 Wakeham and McNichol, 2014). Fernandes et al. (2018) detected similar, though less  
430 pronounced, trends in sediments collected from the Pakistan margin. An increase in  $\delta^{13}\text{C}$  with  
431 enhanced degradation, i.e.  $^{13}\text{C}$ -enriched sediments vs. depleted POM, was also observed in the  
432 South China Sea (Liu et al., 2007), and in the Eastern Tropical North Pacific (Jeffrey et al.,  
433 1983).

434 Despite its common occurrence in OMZ settings, this trend is unusual and, at present, not  
435 explained: degradation of organic carbon in marine environments usually preferentially removes  
436 isotopically heavy carbon (Hatch and Leventhal, 1997), causing a depletion in  $\delta^{13}\text{C}$  with  
437 increased degradation of the sediment. This can be due to the removal of the more labile marine  
438 carbon, and subsequent relative enrichment of terrigenous organic material of a lower initial  
439 reactivity and lower  $\delta^{13}\text{C}$  values (Huguet et al., 2008; Middelburg et al., 1993). However,  
440 progressive depletion also occurs in areas with purely marine input; this is due to preferential  
441 loss of  $^{13}\text{C}$ -enriched carbohydrates over the more  $^{13}\text{C}$ -depleted lipids, and preferential  
442 degradation of easily accessible material over biopolymers (Spiker and Hatcher, 1987), and  
443 polymerization and elimination of functional groups (Galimov, 1988; Balabane et al., 1987).  
444 Conversely, sulfurization, a process observed in euxinic settings appears to preferentially  
445 preserve  $^{13}\text{C}$ -enriched material such as carbohydrates (Van Kaam-Peters et al., 1998); however,  
446 this process is not expected to occur here - the Arabian Sea is anoxic but not sulfidic (Ulloa et  
447 al., 2012) and has not experienced euxinia for the past 120 ka (Schennau et al., 2002).

Nonetheless, in Arabian Sea sediment,  $\delta^{13}\text{C}_{\text{org}}$  values increased by 1.8 ‰ with increasing oxygen exposure time and thus increasing degradation; at the same time, organic carbon contents decreased from 60 to 10 mg g dw<sup>-1</sup>, indicating progressing remineralization (Fig. 1c, Lenger et al., 2014). Cowie (2005) attributed this to the contribution of – potentially – organic matter from the facultatively autotrophic, chemosynthetic sulfur-bacterium *Thioploca* sp., which has been observed in the Arabian Sea (Schmaljohann et al., 2001). However, *Thioploca* sp. has only been reported for shelf and upper slope sediments in the Arabian Sea (above and upper part of OMZ), and it is unlikely that the sulfur-dependent *Thioploca* sp. could have caused this significant depletion by chemoautotrophy, as sulfide concentrations are negligible within the OMZ (Kraal et al., 2012), and there is no evidence for the production of severely <sup>13</sup>C-depleted biomass by filamentous sulfur bacteria (Zhang et al., 2005). Further, the depletion is not only observed in sediments, but also in particle fluxes (Wakeham and McNichol, 2014), which strongly suggests the exclusion of sedimentary sources for <sup>13</sup>C-depleted organic matter. This is also supported by the  $\delta^{13}\text{C}_{\text{org}}$  values of the suspended particulate matter (Fig. S1), which becomes gradually more depleted with depth.

An active nitrogen-cycle in the water column within the Arabian Sea OMZ is undisputedly present, with heterotrophic denitrifying bacteria, nitrifying archaea, nitrite-oxidising and anammox bacteria present in high abundances (Lüke et al., 2016; Villanueva et al., 2014). The <sup>13</sup>C fractionation for the carbon fixation pathways employed by nitrifying archaea (3-Hydroxypropionate/4-Hydroxybutyrate, 3-HP/4-HB) is similar to that of phytoplankton using Rubisco (Könneke et al., 2012). The biomass of heterotrophic denitrifiers is close to the value of the source organic matter (1 ‰ more enriched; Hayes, 2001), and the biochemical pathway employed by nitrite oxidisers (reverse TCA cycle) produces <sup>13</sup>C-enriched biomass (Pearson, 2010). Anammox bacteria, however, are abundant and active in the Arabian Sea (Jensen et al., 2011) and known to produce highly <sup>13</sup>C-depleted biomass by inorganic carbon fixation (Schouten et al., 2004). Anammox bacteria, and other, yet undescribed chemoautotrophs, could thus present a potential pathway for addition of <sup>13</sup>C-depleted organic matter to sinking organic matter, a hypothesis we explore further below.

The water-column derived <sup>13</sup>C-depleted BHT', in combination with the unusual  $\delta^{13}\text{C}_{\text{org}}$  trends, suggests that there may be a substantial contribution of <sup>13</sup>C depleted organic carbon, produced by anammox bacteria, to the sedimentary organic matter. Based on BHT'  $\delta^{13}\text{C}$  values determined in this study, and the fractionation factor associated with anammox lipid biosynthesis of 16 ‰ (lipid versus total biomass; Schouten et al., 2004), we can estimate a  $\delta^{13}\text{C}$  value for anammox biomass: of ca. -28.6 ± 6 ‰, which is similar to the expected value calculated from  $\varepsilon_{\text{biomass-DIC}}$  (22–26 ‰; Schouten et al., 2004) and the generally observed DIC value in the Arabian Sea OMZ at depth, 0 ‰ (Moos, 2000). This is significantly depleted compared to phytoplankton biomass in the Arabian Sea (-19.8 ‰, Fontugne and Duplessy, 1978), and would add depleted organic carbon to the sinking POM.

We modelled the contribution of anammox biomass ( $\chi_{\text{anammox}}$ ) to SOM using an isotopic mass balance approach (using IsoError; Phillips et al., 2005), which employs uncertainty propagation and error estimates and allows the determination of contributions of likely sources of organic matter to the sediment. The end member value of -19.8 ± 0.5 ‰ was used for phytoplankton-derived SOM (Fontugne and Duplessy, 1986; Ziegler et al., 2008). This value is slightly lower than the -19 ‰ observed from the surface particulate carbon, but is representative of sedimentary organic matter, as it accounts for the decreased  $\delta^{13}\text{C}$  values of POM caused by

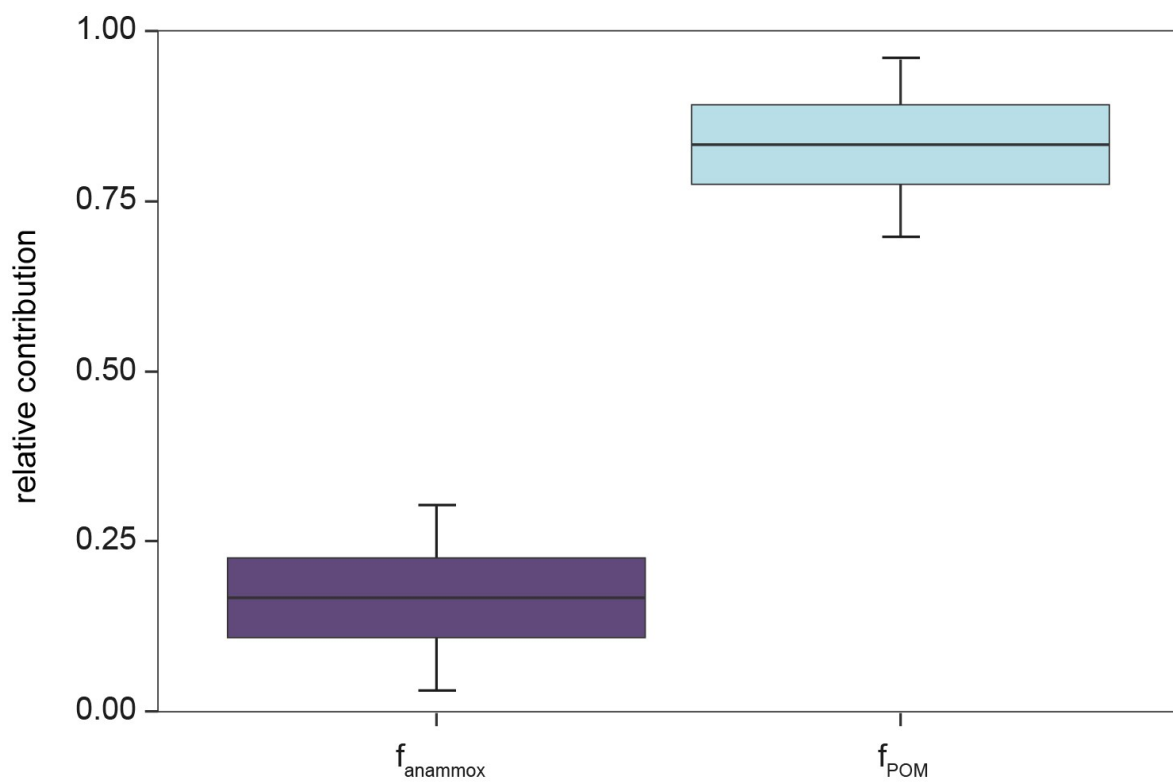
493 degradation of  $^{13}\text{C}$  enriched compounds such as carbohydrates (Close, 2019; Ziegler et al.,  
494 2008). More recent values for phytoplankton  $\delta^{13}\text{C}$  are, to the best of our knowledge, not  
495 available. Planktonic, sinking organic matter, and organic material produced by heterotrophs also  
496 contribute to sedimentary OM. However, this OM value would likely be similar to the organic  
497 matter assimilated (Blair et al., 1985; 2001).  $-28.6 \pm 6\text{\textperthousand}$  was used for anammox-derived organic  
498 carbon, as derived from the  $\delta^{13}\text{C}$  value of BHT' and  $\varepsilon_{\text{bm/lipid}}$  of  $16 \pm 4\text{\textperthousand}$  (Schouten et al., 2004;  
499 Table 1; uncertainty represents combined standard deviations of  $\delta^{13}\text{C}_{\text{BHT}'}$  and  $\varepsilon_{\text{lipid/bm}}$ ). The  $\delta^{13}\text{C}$   
500 value  $-21.5\text{\textperthousand}$  of surface sediment  $\text{C}_{\text{org}}$  in the OMZ was used as the value of the mixture (Table  
501 1):

502

$$\chi_{\text{anammox}} \cdot \delta^{13}\text{C}_{\text{anammox}} + \chi_{\text{PP}} \cdot \delta^{13}\text{C}_{\text{PP}} = -21.5\text{\textperthousand} \quad \text{Eqn 1}$$

503

504 The modelling, assuming the above end member contributions and their statistical uncertainties,  
505 yields a proportion of anammox with a mean of approximately 17% (Fig. 5), and confirms that,  
506 with 95% confidence, anammox contribution to the sedimentary organic matter is between 3 and  
507 30% among the different cores. This suggests that some of the sedimentary organic matter  
508 (SOM) present at P900 is anammox-derived. However, other chemoautotrophic bacteria also  
509 present, or suspected to be present, in the Arabian Sea OMZ (e.g. ammonia-oxidizing archaea,  
510 Pitcher et al., 2011) possess metabolisms which would lead to different  $\delta^{13}\text{C}$  values, and could  
511 therefore be diluting this signal (Hayes, 2001; Pearson, 2010). These results suggest that the  
512 contribution of prokaryotic organic material produced in the OMZ to SOM is larger than  
513 estimated in this simple, two-component mass balance. A three-source model resolving  
514 heterotrophic bacteria or degraded OM, anammox bacteria and phytoplankton was solved with  
515 SIAR (Parnell et al., 2010) and yielded similar results (not shown).



518 **Figure 5.** Results from the isotope mass balance model, showing the calculated means, standard  
519 error, and confidence intervals for contribution from anammox, and planktonic-derived OM  
520 (POM) to the surface sediment at P900.

521

522 This estimate, at a first glance, appears large. However, we can convert experimental  
523 rates of anammox-mediated ammonia oxidation of 27 – 38 nmol L<sup>-1</sup> d<sup>-1</sup> as determined in the  
524 Arabian Sea (Jensen et al., 2011) and alternative rates of 0.24 – 4.32 nmol L<sup>-1</sup> d<sup>-1</sup> estimated by  
525 Ward et al. (2009), to carbon fixed using stoichiometric rates determined for anammox bacteria  
526 of 0.07 mol C mol N<sub>2</sub><sup>-1</sup> (Jetten et al., 2001; Strous et al., 1999; van de Vossenberg et al., 2008).  
527 Assuming a production depth of 300 to 900 m water depth, with a maximum at 600 m (Pitcher et  
528 al., 2011), anammox production over the whole depth could be estimated using Equation 2 (see  
529 Fig. S5),

530

$$P = \frac{(k \cdot 600)}{2} \quad \text{Eqn. 2}$$

531

532 in which  $k$  corresponds to maximum rate at maximum production depth calculated from  
533 aforementioned published anammox rates ( $k$  equals 138.7 – 9855 μmol m<sup>-3</sup> yr<sup>-1</sup>, Jensen et al.  
534 2011; 87.6 – 1576.8 μmol m<sup>-3</sup> yr<sup>-1</sup>, Ward et al. 2009; Fig. S5).

536 Using this equation, we calculated that water-column anammox bacteria produce up to  
537 3.5 g organic C m<sup>-2</sup> yr<sup>-1</sup>. These estimates dwarf sedimentary anammox rates, with C-fixation  
538 determined to be at 64 pg organic C m<sup>-2</sup> yr<sup>-1</sup> in the Arabian Sea (Sokoll et al., 2012), indicating  
539 that most of the anammox carbon in the sediment is water-column derived. Given organic carbon  
540 accumulation rates (Lengger et al., 2012b) of 3 to 5 g C m<sup>-2</sup> yr<sup>-1</sup> at P900 and assuming a 17 %  
541 anammox contribution to sedimentary organic matter, a maximum of 24 % of annually produced,  
542 water-column anammox biomass is preserved in this anoxic setting. Within the sediment from  
543 the OMZ, as seen from a sedimentary depth profile at P900 in the OMZ (Fig. 3), δ<sup>13</sup>C<sub>org</sub> also  
544 shifts to higher values with depth, to a maximum of -20.8 ‰ at 8 cmbsf. However, contrary to  
545 oxic degradation, no decrease in SOM contents occurs over the first 14 cm (Fig. 3). In this case,  
546 the increase in δ<sup>13</sup>C<sub>org</sub> likely reflects input by other sedimentary autotrophs, producing enriched  
547 organic carbon. This suggests that the <sup>13</sup>C-depleted SOM signal from the OMZ is not completely  
548 preserved.

549 Other chemoautotrophs, where specific biomarkers are not available, could also  
550 contribute to the SOM: at depth, the increased availability of CO<sub>2</sub> derived from heterotrophic  
551 respiration of the POM pool would result in greater discrimination against <sup>13</sup>C (Freeman et al.,  
552 1994; Freeman, 2001). An example are lipids of ammonia-oxidising archaea, which were more  
553 depleted when deposited in the OMZ than below the OMZ (Table S2), suggesting that some of  
554 those were produced in the produced in the OMZ and transported to the sediment (Lengger et al.,  
555 2014, 2012b; Schouten et al., 2012).. However, as these archaeal lipids present a mixed pelagic  
556 and sedimentary signal, quantitative estimates are not possible.

557 Hence, chemoautotrophic carbon fixation could explain the low δ<sup>13</sup>C values of  
558 sedimentary OM observed within the OMZ. As the newly produced organic carbon is more  
559 labile than surface-produced organic matter, it would degrade more quickly upon exposure to

560 oxic bottom waters. This poorer preservation of anammox biomass results in a shift back towards  
561 the  $^{13}\text{C}$  signature of the primary photosynthetic production, which is observed as the enrichment  
562 in sedimentary  $\delta^{13}\text{C}_{\text{org}}$  with increasing oxygen exposure times (Fig. 1e). A likely explanation for  
563 this lability of anammox biomass is that, due to the lack of zooplankton in the OMZ, this organic  
564 matter is not fecal-pellet packaged or adsorbed to inorganic particles and thus not matrix  
565 protected (cf. Burdige, 2007). Wakeham et al. (2002) analysed the biomarker fluxes in sinking  
566 particles in the Arabian Sea, and they also found that surface-produced lipids such as alkenones  
567 (which would be fecal pellet packaged) were exceptionally well-preserved compared to the total  
568 organic carbon of the SPM. Gong and Hollander (1997) also noted an enhanced contribution of  
569 bacterial biomass to sediment deposited under anoxic conditions in the Santa Monica Basin,  
570 when compared to sediment located in nearby oxygenated bottom waters. Studies examining  
571 carbon fluxes in the Arabian Sea (Keil et al., 2016) and the Cariaco basin (Taylor et al., 2001)  
572 invoked the addition of chemotrophic derived carbon from a midwater source in order to  
573 explain the enhanced carbon fluxes observed, even if oxygen depletion and other factors such as  
574 the lack of zooplankton were taken into account.

575  
576 4.3. Quantifying the biological pump and remineralization rates

577 Models of the biological pump consider primary production, particle fluxes, oxygen  
578 concentrations, and respiratory rates. Sinking organic matter is traditionally regarded as a  
579 reflection of exported organic material from the photic zone, and export models consider  
580 remineralization and C-loss (Cabré et al., 2015; Schlitzer, 2002), based on claims that bacterial  
581 contributions do not sink (Buesseler et al., 2007). However, relying on these parameters,  
582 estimates of particulate organic carbon flux in the Arabian Sea are generally too low to sustain  
583 experimentally observed denitrification, bacterial production, and oxygen deficiency in the  
584 Arabian Sea (Anderson and Ryabchenko, 2009; Andrews et al., 2017; Naqvi and Shailaja, 1993;  
585 Rixen and Ittekkot, 2005). New mechanisms have been discovered that can explain downward  
586 transport of smaller particles and bacteria, such as particle aggregation (Burd and Jackson, 2009),  
587 and mixed layer transport mechanisms (Bol et al., 2018), which enable the consideration of the  
588 contribution of anammox biomass to sinking OM.

589 In previous work, the deficit in modelled and observed C-utilization estimated from  
590 denitrification was as high as  $70 \text{ g C m}^{-2} \text{ y}^{-1}$  (Naqvi and Shailaja, 1993). Including anammox in  
591 models of the nitrogen cycle can account for at least 30% or more of the nitrogen losses, as well  
592 as accounting for organic carbon production, thereby reconciling some of this budget  
593 discrepancy. More recently, the combined inclusion of mesopelagic zooplankton and  
594 heterotrophic bacteria into 3D models resulted in much lower bacterial productivity ( $4.7 \text{ g C m}^{-2}$   
595  $\text{y}^{-1}$ ) than observational estimates of  $10.4 \text{ g C m}^{-2} \text{ y}^{-1}$  (Anderson and Ryabchenko, 2009). Other  
596 recent models, combined with experimental observations of particle fluxes, suggest that at some  
597 stations, the lower oxycline is associated with  $0.4$  to  $1.8 \text{ g C m}^{-2} \text{ y}^{-1}$  increases in net carbon fluxes  
598 (Roullier et al., 2014). Horizontal transport, also from nepheloid layers, novel transport  
599 mechanisms from the mixed layer, and DOM, have previously been invoked as the missing  
600 carbon supply. Here, we estimate that an additional  $3.5 \text{ g m}^{-2} \text{ y}^{-1}$  of organic carbon are produced  
601 by anammox from DIC, with other chemotrophic processes possibly adding to this estimate.  
602 This also affects estimates of nitrogen losses and has direct implications for the forecasting of  
603 OMZs in a warming world.

In paleoceanography, the  $\delta^{13}\text{C}$  values of total organic carbon are commonly used in combination with organic carbon contents in sediment cores to interpret changes in sea surface biogeochemistry and to discern the causes for ocean deoxygenation (Jenkyns, 2010; Meyers, 2014). Negative  $\delta^{13}\text{C}$  excursions are associated with either atmospheric injection of depleted CO<sub>2</sub> and/or increased CO<sub>2</sub> availability (Pagani, 2005; Pancost and Pagani, 2005), or a higher input of terrigenous organic matter. Positive excursions are inferred to reflect increased burial rates of organic carbon, i.e. the removal of ‘light’ carbon from the ocean-atmosphere reservoir (e.g. Kuypers et al., 2002; Jenkyns, 1985). An increase in TOC coinciding with a negative carbon isotope excursion has been observed in the sedimentary record numerous times. They are a prominent feature in OAE 1a (Leckie et al., 2002), during the PETM (Zachos et al., 2005), and in the Eastern Mediterranean during Sapropel deposition (Meyers and Arnaboldi, 2008). Our results show that if non-sulfidic OMZs expand to impinge on the sediment, a significant amount of  $^{13}\text{C}$ -depleted organic carbon can be preserved, changing the carbon isotope composition of organic matter by up to – 1.6 ‰ in the case of Arabian Sea surface sediments, and by -0.5 to -1 ‰ in deeper sediments. When evaluating past events based on bulk  $\delta^{13}\text{C}$  values, the incorporation of chemoautotrophically produced carbon must thus be considered. This also further supports claims that calculations of pCO<sub>2</sub> based on differences between  $\delta^{13}\text{C}$  of organic and inorganic carbon should not rely on bulk organic carbon that includes bacterial contributions, but instead use compound specific  $\delta^{13}\text{C}$  values derived from algae, consistent with previous investigations (Pancost et al., 1999; Pancost et al., 2013; reviewed by Witkowski et al., 2018). By extension, a deviation from the relationship between  $\delta^{13}\text{C}$  bulk OM and  $\delta^{13}\text{C}$  phytane could be an indicator for the chemoautotrophic contribution to sedimentary OM.

Chemoautotrophic metabolism in euxinic water columns, where often very low  $\delta^{13}\text{C}_{\text{DIC}}$  values are observed (van Breugel et al., 2005a,b; Fry et al., 1991; Volkov, 2000), has previously been invoked as contributing to organic matter in these setting. Anammox, which has been shown to be an important process in the anoxic water column overlying euxinia (Kuypers et al., 2003), also needs to be considered. Anammox also plays an important role in the nitrogen cycle of Mediterranean sapropel events, even in sapropels where euxinia appears to have occurred (Rush et al., 2019), potentially causing a significant contribution of anammox to the depleted  $\delta^{13}\text{C}_{\text{org}}$  values of these sapropels. Previously, a conceptual model invoking chemoautotrophy has been invoked to explain e.g. the End-Permian (Luo et al., 2014) and the Lomagundi isotope excursion (Bekker et al., 2008).

Settings similar to the Arabian Sea, with  $\leq 4.5 \mu\text{mol kg}^{-1} \text{O}_2$ , occur in the East Pacific and those settings in total occupy an area of  $8.45 \text{ to } 15 \times 10^{12} \text{ m}^2$  (Karstensen et al., 2008; Hattori, 1983; Paulmier and Ruiz-Pino, 2009), or a volume of  $0.46 \times 10^{15} \text{ m}^3$  with  $1.148 \times 10^{12} \text{ m}^2$  in contact with the sediment (Helly and Levin, 2004). OMZs are expanding in size and in volume (Stramma et al., 2010; Queste et al., 2018), and anammox bacteria play a key role in these settings, particularly because they tolerate higher oxygen concentrations than denitrifiers (Dalsgaard et al., 2014). The labile organic matter added to the sinking carbon can fuel heterotrophic processes, further exacerbating oxygen depletion, and nitrogen loss by denitrification. For accurate future forecasting, it is imperative to reconcile experimental and model-based estimates. Novel, detailed observations explaining the vertical transport of bacterial biomass, and evidence from the isotopic composition of TOC and biomarkers for chemoautotrophic processes, such as shown here for anammox, will enable the further unravelling of the biogeochemical mechanisms underpinning present, past, and future OMZs.

649 **5 Conclusions**

650 Combining the  $\delta^{13}\text{C}$  values of BHT', a biomarker from anammox bacteria, and the  $\delta^{13}\text{C}$   
651 values of sedimentary organic matter allowed us to estimate the contribution of anammox to  
652 SOM in the Arabian Sea. This can be as much as 30 % of organic matter deposited within the  
653 OMZ. In the sediments underlying the Arabian Sea,  $\delta^{13}\text{C}$  values of total organic matter can shift  
654 by 1 to 2 ‰ due to these bacterial contributions, but it remains unclear how well and under what  
655 conditions this signature is preserved. Our results suggest that chemoautotrophs (e.g. anammox  
656 bacteria) contribute more than previously believed to the burial of carbon in oxygen deficient  
657 zones, and remineralization rates are potentially higher than inferred from organic matter  
658 decreases. This implies that, when past occurrences of OMZs are evaluated based on  $\delta^{13}\text{C}$  values  
659 of SOM, a  $^{13}\text{C}$ -depleted contribution of bacteria needs to be considered. Chemoautotrophic  
660 carbon fixation thus represents a mechanism of  $\text{CO}_2$  removal from the pelagic water column, and  
661 contributes to fluxes of sinking organic carbon. It explains some of the mismatches in carbon  
662 budgets when experimental and modelling estimates are compared - and it should therefore be  
663 included in biogeochemical models predicting feedbacks to a warming world.

664

665 **Acknowledgements:** SKL was supported by Rubicon fellowship nr. 825.14.014 from the  
666 Netherlands Organization for Scientific Research (NWO). MJ, JJM, JSSD, and SS were  
667 supported by NESSC OCW/NWO 024 002.001 and MJ, JSSD and DR by SIAM OCW/NWO  
668 024 002.002 grants. RSN and DR were supported by NERC grant ANAMMARKS  
669 NE/N011112/1 awarded to DR. JB is supported by a NERC GW4+ Doctoral Training  
670 Partnership studentship from the Natural Environment Research Council (NE/L002434/1) and is  
671 thankful for the support and additional funding from CASE partner, Elementar UK Ltd. We  
672 thank Guylaine Nijtten (Radboud University) for maintaining the Scalindua biomass over the  
673 years. We thank Ian Bull and Alison Kuhl for support with instrumentation, and Jort Ossebaar  
674 and Kevin Donkers for support with TOC and bulk isotope analysis. We would also like to  
675 acknowledge the shipboard party of 64PE306, in particular chief scientist Gert-Jan Reichart, and  
676 Leon Moodley and Lara Pozzato, who provided us with samples from their incubation  
677 experiments. The associate editor S. Mikaloff-Fletcher and the referees, K. Freeman and A.  
678 Singh are thanked for their highly valued contributions to improving this manuscript.

679

680 **Data statement: Data statement:** All supporting data is included, and will be deposited on  
681 Pangaea as appropriate.

682

683

684 **References**

- 685 Anderson, T. R., & Ryabchenko, V. A. (2009). Carbon cycling in the Mesopelagic Zone of the  
686 central Arabian Sea: Results from a simple model. *Washington DC American Geophysical Union*  
687 *Geophysical Monograph Series*, 185, 281–297. <https://doi.org/10.1029/2007GM000686>
- 688 Andrews, O., Buitenhuis, E., Le Quéré, C., & Suntharalingam, P. (2017). Biogeochemical  
689 modelling of dissolved oxygen in a changing ocean. *Philosophical Transactions of the Royal*  
690 *Society A: Mathematical, Physical and Engineering Sciences*, 375(2102), 20160328.  
691 <https://doi.org/10.1098/rsta.2016.0328>
- 692 Angelis, Y. S., Kioussi, M. K., Kiousi, P., Brenna, J. T., & Georgakopoulos, C. G. (2012).  
693 Examination of the kinetic isotopic effect to the acetylation derivatization for the gas  
694 chromatographic-combustion-isotope ratio mass spectrometric doping control analysis of  
695 endogenous steroids: Kinetic isotopic effect to the acetylation derivatization of endogenous  
696 steroids. *Drug Testing and Analysis*, 4(12), 923–927. <https://doi.org/10.1002/dta.408>
- 697 Balabane, M., Galimov, E., Hermann, M., & Létolle, R. (1987). Hydrogen and carbon isotope  
698 fractionation during experimental production of bacterial methane. *Organic Geochemistry*, 11(2),  
699 115–119. [https://doi.org/10.1016/0146-6380\(87\)90033-7](https://doi.org/10.1016/0146-6380(87)90033-7)
- 700 Bekker, A., Holmden, C., Beukes, N. J., Kenig, F., Eglington, B., & Patterson, W. P. (2008).  
701 Fractionation between inorganic and organic carbon during the Lomagundi (2.22–2.1 Ga) carbon  
702 isotope excursion. *Earth and Planetary Science Letters*, 271(1), 278–291.  
703 <https://doi.org/10.1016/j.epsl.2008.04.021>
- 704 Blair, N., Leu, A., Muñoz, E., Olsen, J., Kwong, E., & Marais, D. D. (1985). Carbon isotopic  
705 fractionation in heterotrophic microbial metabolism. *Applied and Environmental Microbiology*,  
706 50(4), 996–1001.
- 707 Bol, R., Henson, S. A., Rumyantseva, A., & Briggs, N. (2018). High-Frequency Variability of  
708 Small-Particle Carbon Export Flux in the Northeast Atlantic. *Global Biogeochemical Cycles*,  
709 32(12), 1803–1814. <https://doi.org/10.1029/2018GB005963>
- 710 Breitburg, D., Levin, L. A., Oschlies, A., Grégoire, M., Chavez, F. P., Conley, D. J., et al.  
711 (2018). Declining oxygen in the global ocean and coastal waters. *Science*, 359(6371), eaam7240.  
712 <https://doi.org/10.1126/science.aam7240>
- 713 van Breugel, Y., Schouten, S., Paetzel, M., Nordeide, R., & Sinninghe Damsté, J. S. (2005a).  
714 The impact of recycling of organic carbon on the stable carbon isotopic composition of dissolved  
715 inorganic carbon in a stratified marine system (Kyllaren fjord, Norway). *Organic Geochemistry*,  
716 36(8), 1163–1173. <https://doi.org/10.1016/j.orggeochem.2005.03.003>

- 717 van Breugel, Y., Schouten, S., Paetzel, M., Ossebaar, J., & Sinninghe Damsté, J. S. (2005b).  
718 Reconstruction of  $\delta^{13}\text{C}$  of chemocline  $\text{CO}_2$  (aq) in past oceans and lakes using the  $\delta^{13}\text{C}$  of fossil  
719 isorenieratene. *Earth and Planetary Science Letters*, 235(1), 421–434.  
720 <https://doi.org/10.1016/j.epsl.2005.04.017>
- 721 Buesseler, K. O., Antia, A. N., Chen, M., Fowler, S. W., Gardner, W. D., Gustafsson, O., et al.  
722 (2007). An assessment of the use of sediment traps for estimating upper ocean particle fluxes.  
723 *Journal of Marine Research*, 65(3), 345–416. <https://doi.org/10.1357/002224007781567621>
- 724 Burd, A. B., & Jackson, G. A. (2009). Particle Aggregation. *Annual Review of Marine Science*,  
725 1(1), 65–90. <https://doi.org/10.1146/annurev.marine.010908.163904> Burdige, D. J. (2007).  
726 Preservation of Organic Matter in Marine Sediments: Controls, Mechanisms, and an Imbalance  
727 in Sediment Organic Carbon Budgets? *Chemical Reviews*, 107(2), 467–485.  
728 <https://doi.org/10.1021/cr050347q>
- 729 Cabré, A., Marinov, I., Bernardello, R., & Bianchi, D. (2015). Oxygen minimum zones in the  
730 tropical Pacific across CMIP5 models: mean state differences and climate change trends.  
731 *Biogeosciences*, 12(18), 5429–5454. <https://doi.org/10.5194/bg-12-5429-2015>
- 732 Canfield, D. E. (2006). Models of oxic respiration, denitrification and sulfate reduction in zones  
733 of coastal upwelling. *Geochimica et Cosmochimica Acta*, 70(23), 5753–5765.  
734 <https://doi.org/10.1016/j.gca.2006.07.023>
- 735 Close, H. G. (2019). Compound-Specific Isotope Geochemistry in the Ocean. *Annual Review of  
736 Marine Science*, 11(1), 27–56. <https://doi.org/10.1146/annurev-marine-121916-063634>
- 737 Cooke, M. P., Talbot, H. M., & Farrimond, P. (2008). Bacterial populations recorded in  
738 bacteriohopanepolyol distributions in soils from Northern England. *Organic Geochemistry*,  
739 39(9), 1347–1358. <https://doi.org/10.1016/j.orggeochem.2008.05.003>
- 740 Cooke, M. P., van Dongen, B. E., Talbot, H. M., Semiletov, I., Shakhova, N., Guo, L., &  
741 Gustafsson, Ö. (2009). Bacteriohopanepolyol biomarker composition of organic matter exported  
742 to the Arctic Ocean by seven of the major Arctic rivers. *Organic Geochemistry*, 40(11), 1151–  
743 1159. <https://doi.org/10.1016/j.orggeochem.2009.07.014>
- 744 Cowie, G. (2005). The biogeochemistry of Arabian Sea surficial sediments: A review of recent  
745 studies. *Progress in Oceanography*, 65(2), 260–289.  
746 <https://doi.org/10.1016/j.pocean.2005.03.003>
- 747 Cowie, G. L., & Hedges, J. I. (1992). Sources and reactivities of amino acids in a coastal marine  
748 environment. *Limnology and Oceanography*, 37(4), 703–724.  
749 <https://doi.org/10.4319/lo.1992.37.4.0703>
- 750 Cowie, G. L., Calvert, S. E., Pedersen, T. F., Schulz, H., & von Rad, U. (1999). Organic content  
751 and preservational controls in surficial shelf and slope sediments from the Arabian Sea (Pakistan  
752 margin). *Marine Geology*, 161(1), 23–38. [https://doi.org/10.1016/S0025-3227\(99\)00053-5](https://doi.org/10.1016/S0025-3227(99)00053-5)

- 753 Cowie, G. L., Mowbray, S., Lewis, M., Matheson, H., & McKenzie, R. (2009). Carbon and  
754 nitrogen elemental and stable isotopic compositions of surficial sediments from the Pakistan  
755 margin of the Arabian Sea. *Deep Sea Research Part II: Topical Studies in Oceanography*, 56(6),  
756 271–282. <https://doi.org/10.1016/j.dsr2.2008.05.031>
- 757 Dalsgaard, T., Stewart, F. J., Thamdrup, B., Brabandere, L. D., Revsbech, N. P., Ulloa, O., et al.  
758 (2014). Oxygen at Nanomolar Levels Reversibly Suppresses Process Rates and Gene Expression  
759 in Anammox and Denitrification in the Oxygen Minimum Zone off Northern Chile. *MBio*, 5(6),  
760 e01966-14. <https://doi.org/10.1128/mBio.01966-14>
- 761 Devol, A. H. (2015). Denitrification, Anammox, and N<sub>2</sub> Production in Marine Sediments.  
762 *Annual Review of Marine Science*, 7(1), 403–423. <https://doi.org/10.1146/annurev-marine-010213-135040>
- 764 Dunne, J. P., Sarmiento, J. L., & Gnanadesikan, A. (2007). A synthesis of global particle export  
765 from the surface ocean and cycling through the ocean interior and on the seafloor. *Global  
766 Biogeochemical Cycles*, 21(4). <https://doi.org/10.1029/2006GB002907>
- 767 Fernandes, S., Mazumdar, A., Bhattacharya, S., Peketi, A., Mapder, T., Roy, R., et al. (2018).  
768 Enhanced carbon-sulfur cycling in the sediments of Arabian Sea oxygen minimum zone center.  
769 *Scientific Reports*, 8(1), 8665. <https://doi.org/10.1038/s41598-018-27002-2>
- 770 Fischer, W. W., Summons, R. E., & Pearson, A. (2005). Targeted genomic detection of  
771 biosynthetic pathways: anaerobic production of hopanoid biomarkers by a common sedimentary  
772 microbe. *Geobiology*, 3(1), 33–40. <https://doi.org/10.1111/j.1472-4669.2005.00041.x>
- 773 Fontugne, M., & Duplessy, J. C. (1978). Carbon isotope ratio of marine plankton related to  
774 surface water masses. *Earth and Planetary Science Letters*, 41(3), 365–371.  
775 [https://doi.org/10.1016/0012-821X\(78\)90191-7](https://doi.org/10.1016/0012-821X(78)90191-7)
- 776 Fontugne, M. R., & Duplessy, J.-C. (1986). Variations of the monsoon regime during the upper  
777 quaternary: Evidence from carbon isotopic record of organic matter in North Indian Ocean  
778 sediment cores. *Palaeogeography, Palaeoclimatology, Palaeoecology*, 56(1), 69–88.  
779 [https://doi.org/10.1016/0031-0182\(86\)90108-2](https://doi.org/10.1016/0031-0182(86)90108-2)
- 780 Freeman, K. H. (2001). Isotopic Biogeochemistry of Marine Organic Carbon. *Reviews in  
781 Mineralogy and Geochemistry*, 43(1), 579–605. <https://doi.org/10.2138/gsrmg.43.1.579>
- 782 Freeman, K. H., Wakeham, S. G., & Hayes, J. M. (1994). Predictive isotopic biogeochemistry:  
783 Hydrocarbons from anoxic marine basins. *Organic Geochemistry*, 21(6), 629–644.  
784 [https://doi.org/10.1016/0146-6380\(94\)90009-4](https://doi.org/10.1016/0146-6380(94)90009-4)
- 785 Fry, B., Jannasch, H. W., Molyneaux, S. J., Wirsen, C. O., Muramoto, J. A., & King, S. (1991).  
786 Stable isotope studies of the carbon, nitrogen and sulfur cycles in the Black Sea and the Cariaco  
787 Trench. *Deep Sea Research Part A. Oceanographic Research Papers*, 38, S1003–S1019.  
788 [https://doi.org/10.1016/S0198-0149\(10\)80021-4](https://doi.org/10.1016/S0198-0149(10)80021-4)

- 789 Galimov, E. M. (1988). Sources and mechanisms of formation of gaseous hydrocarbons in  
790 sedimentary rocks. *Chemical Geology*, 71(1), 77–95. [https://doi.org/10.1016/0009-2541\(88\)90107-6](https://doi.org/10.1016/0009-2541(88)90107-6)
- 792 Gong, C., & Hollander, D. J. (1997). Differential contribution of bacteria to sedimentary organic  
793 matter in oxic and anoxic environments, Santa Monica Basin, California. *Organic Geochemistry*,  
794 26(9), 545–563. [https://doi.org/10.1016/S0146-6380\(97\)00018-1](https://doi.org/10.1016/S0146-6380(97)00018-1)
- 795 Härtner, T., Straub, K. L., & Kannenberg, E. (2005). Occurrence of hopanoid lipids in anaerobic  
796 Geobacter species. *FEMS Microbiology Letters*, 243(1), 59–64.  
797 <https://doi.org/10.1016/j.femsle.2004.11.039>
- 798 Hartnett, H. E., Keil, R. G., Hedges, J. I., & Devol, A. H. (1998). Influence of oxygen exposure  
799 time on organic carbon preservation in continental margin sediments. *Nature*, 391(6667), 572–  
800 575. <https://doi.org/10.1038/35351>
- 801 Hatch, J. R., & Leventhal, J. S. (1997). Early diagenetic partial oxidation of organic matter and  
802 sulfides in the Middle Pennsylvanian (Desmoinesian) Excello Shale member of the Fort Scott  
803 Limestone and equivalents, northern Midcontinent region, USA. *Chemical Geology*, 134(4),  
804 215–235. [https://doi.org/10.1016/S0009-2541\(96\)00006-X](https://doi.org/10.1016/S0009-2541(96)00006-X)
- 805 Hayes, J. M. (2001). Fractionation of Carbon and Hydrogen Isotopes in Biosynthetic Processes.  
806 *Reviews in Mineralogy and Geochemistry*, 43(1), 225–277.  
807 <https://doi.org/10.2138/gsrmg.43.1.225>
- 808 Hedges, J. I., & Keil, R. G. (1995). Sedimentary organic matter preservation: an assessment and  
809 speculative synthesis. *Marine Chemistry*, 49(2), 81–115. [https://doi.org/10.1016/0304-4203\(95\)00008-F](https://doi.org/10.1016/0304-4203(95)00008-F)
- 811 Helly, J. J., & Levin, L. A. (2004). Global distribution of naturally occurring marine hypoxia on  
812 continental margins. *Deep Sea Research Part I: Oceanographic Research Papers*, 51(9), 1159–  
813 1168. <https://doi.org/10.1016/j.dsr.2004.03.009>
- 814 Herndl, G. J., & Reinthal, T. (2013). Microbial control of the dark end of the biological pump. *Nature Geoscience*, 6(9), 718–724.  
815 <https://doi.org/10.1038/ngeo1921>
- 816 Hollander, D. J., & Smith, M. A. (2001). Microbially mediated carbon cycling as a control on the  
817  $\delta^{13}\text{C}$  of sedimentary carbon in eutrophic Lake Mendota (USA): new models for interpreting  
818 isotopic excursions in the sedimentary record. *Geochimica et Cosmochimica Acta*, 65(23), 4321–  
819 4337. [https://doi.org/10.1016/S0016-7037\(00\)00506-8](https://doi.org/10.1016/S0016-7037(00)00506-8)
- 820 Huguet, C., de Lange, G. J., Gustafsson, Ö., Middelburg, J. J., Sinninghe Damsté, J. S., &  
821 Schouten, S. (2008). Selective preservation of soil organic matter in oxidized marine sediments  
822 (Madeira Abyssal Plain). *Geochimica et Cosmochimica Acta*, 72(24), 6061–6068.  
823 <https://doi.org/10.1016/j.gca.2008.09.021>

- 824 Jaeschke, A., Ziegler, M., Hopmans, E. C., Reichart, G.-J., Lourens, L. J., Schouten, S., &  
825 Sinninghe Damsté, J. S. (2009). Molecular fossil evidence for anaerobic ammonium oxidation in  
826 the Arabian Sea over the last glacial cycle: Anammox in the Arabian Sea. *Paleoceanography*,  
827 24(2), n/a-n/a. <https://doi.org/10.1029/2008PA001712>
- 828 Jeffrey, A. W. A., Pflaum, R. C., Brooks, J. M., & Sackett, W. M. (1983). Vertical trends in  
829 particulate organic carbon  $^{13}\text{C}$ :  $^{12}\text{C}$  ratios in the upper water column. *Deep Sea Research Part A.*  
830 *Oceanographic Research Papers*, 30(9), 971–983. [https://doi.org/10.1016/0198-0149\(83\)90052-3](https://doi.org/10.1016/0198-0149(83)90052-3)
- 832 Jenkyns, H. C. (1985). The early Toarcian and Cenomanian-Turonian anoxic events in Europe:  
833 comparisons and contrasts. *Geologische Rundschau*, 74(3), 505–518.  
834 <https://doi.org/10.1007/BF01821208>
- 835 Jenkyns, H. C. (2010). Geochemistry of oceanic anoxic events: REVIEW. *Geochemistry,*  
836 *Geophysics, Geosystems*, 11(3). <https://doi.org/10.1029/2009GC002788>
- 837 Jensen, M. M., Lam, P., Revsbech, N. P., Nagel, B., Gaye, B., Jetten, M. S., & Kuyper, M. M.  
838 (2011). Intensive nitrogen loss over the Omani Shelf due to anammox coupled with dissimilatory  
839 nitrite reduction to ammonium. *The ISME Journal*, 5(10), 1660–1670.  
840 <https://doi.org/10.1038/ismej.2011.44>
- 841 Jetten, M. S. M., Wagner, M., Fuerst, J., van Loosdrecht, M., Kuenen, G., & Strous, M. (2001).  
842 Microbiology and application of the anaerobic ammonium oxidation ('anammox') process.  
843 *Current Opinion in Biotechnology*, 12(3), 283–288. [https://doi.org/10.1016/S0958-1669\(00\)00211-1](https://doi.org/10.1016/S0958-1669(00)00211-1)
- 845 Keil, R. G., Neibauer, J. A., Biladeau, C., van der Elst, K., & Devol, A. H. (2016). A multiproxy  
846 approach to understanding the “enhanced” flux of organic matter through the oxygen-deficient  
847 waters of the Arabian Sea. *Biogeosciences*, 13(7), 2077–2092. <https://doi.org/10.5194/bg-13-2077-2016>
- 849 Keil, Richard G., Montluçon, D. B., Prahl, F. G., & Hedges, J. I. (1994). Sorptive preservation of  
850 labile organic matter in marine sediments. *Nature*, 370(6490), 549–552.  
851 <https://doi.org/10.1038/370549a0>
- 852 Kharbush, J. J., Thompson, L. R., Haroon, M. F., Knight, R., & Aluwihare, L. I. (2018).  
853 Hopanoid-producing bacteria in the Red Sea include the major marine nitrite oxidizers. *FEMS*  
854 *Microbiology Ecology*, 94(6). <https://doi.org/10.1093/femsec/fiy063>
- 855 Koho, K. A., Nierop, K. G. J., Moodley, L., Middelburg, J. J., Pozzato, L., Soetaert, K., et al.  
856 (2013). Microbial bioavailability regulates organic matter preservation in marine sediments.  
857 *Biogeosciences*, 10(2), 1131–1141. <https://doi.org/10.5194/bg-10-1131-2013>

- 858 Könneke, M., Lipp, J. S., & Hinrichs, K.-U. (2012). Carbon isotope fractionation by the marine  
859 ammonia-oxidizing archaeon *Nitrosopumilus maritimus*. *Organic Geochemistry*, 48, 21–24.  
860 <https://doi.org/10.1016/j.orggeochem.2012.04.007>
- 861 Köster, J., Rospondek, M., Schouten, S., Kotarba, M., Zubrzycki, A., & Sinninghe Damste, J. S.  
862 (1998). Biomarker geochemistry of a foreland basin: the Oligocene Menilite Formation in the  
863 Flysch Carpathians of Southeast Poland. *Organic Geochemistry*, 29(1), 649–669.  
864 [https://doi.org/10.1016/S0146-6380\(98\)00182-X](https://doi.org/10.1016/S0146-6380(98)00182-X)
- 865  
866 Kroopnick, P. M. (1985). The distribution of  $^{13}\text{C}$  of  $\Sigma\text{CO}_2$  in the world oceans. *Deep Sea*  
867 *Research Part A. Oceanographic Research Papers*, 32(1), 57–84. [https://doi.org/10.1016/0198-0149\(85\)90017-2](https://doi.org/10.1016/0198-0149(85)90017-2)
- 868  
869 Kuypers, M. M. M., Slikkers, A. O., Lavik, G., Schmid, M., Jørgensen, B. B., Kuenen, J. G., et  
870 al. (2003). Anaerobic ammonium oxidation by anammox bacteria in the Black Sea. *Nature*,  
871 422(6932), 608–611. <https://doi.org/10.1038/nature01472>
- 872  
873 Kuypers, Marcel M. M., Pancost, Richard D., Nijenhuis, Ivar A., & Sinninghe Damsté, Jaap S.  
874 (2002). Enhanced productivity led to increased organic carbon burial in the euxinic North  
875 Atlantic basin during the late Cenomanian oceanic anoxic event. *Paleoceanography*, 17(4), 3–1.  
<https://doi.org/10.1029/2000PA000569>
- 876  
877 Lam, P., Lavik, G., Jensen, M. M., van de Vossenberg, J., Schmid, M., Woebken, D., et al.  
878 (2009). Revising the nitrogen cycle in the Peruvian oxygen minimum zone. *Proceedings of the*  
*National Academy of Sciences*, 106(12), 4752–4757. <https://doi.org/10.1073/pnas.0812444106>
- 879  
880 Lam, Phyllis, & Kuypers, M. M. M. (2010). Microbial Nitrogen Cycling Processes in Oxygen  
881 Minimum Zones. *Annual Review of Marine Science*, 3(1), 317–345.  
<https://doi.org/10.1146/annurev-marine-120709-142814>
- 882  
883 Lam, Phyllis, Jensen, M. M., Lavik, G., McGinnis, D. F., Müller, B., Schubert, C. J., et al.  
884 (2007). Linking crenarchaeal and bacterial nitrification to anammox in the Black Sea.  
*Proceedings of the National Academy of Sciences*, 104(17), 7104–7109.  
<https://doi.org/10.1073/pnas.0611081104>
- 885  
886 Leckie, R. M., Bralower, T. J., & Cashman, R. (2002). Oceanic anoxic events and plankton  
887 evolution: Biotic response to tectonic forcing during the mid-Cretaceous. *Paleoceanography*,  
888 17(3), 13-1-13–29. <https://doi.org/10.1029/2001PA000623>
- 889  
890 Lengger, S. K., Hopmans, E. C., Sinninghe Damsté, J. S., & Schouten, S. (2012a). Comparison  
891 of extraction and work up techniques for analysis of core and intact polar tetraether lipids from  
892 sedimentary environments. *Organic Geochemistry*, 47, 34–40.  
<https://doi.org/10.1016/j.orggeochem.2012.02.009>
- 893  
894 Lengger, S. K., Hopmans, E. C., Reichart, G.-J., Nierop, K. G. J., Sinninghe Damsté, J. S., &  
Schouten, S. (2012b). Intact polar and core glycerol dibiphytanyl glycerol tetraether lipids in the

- 895 Arabian Sea oxygen minimum zone. Part II: Selective preservation and degradation in sediments  
896 and consequences for the TEX<sub>86</sub>. *Geochimica et Cosmochimica Acta*, 98, 244–258.  
897 <https://doi.org/10.1016/j.gca.2012.05.003>
- 908 Lengger, S. K., Hopmans, E. C., Sinninghe Damsté, J. S., & Schouten, S. (2014). Impact of  
909 sedimentary degradation and deep water column production on GDGT abundance and  
900 distribution in surface sediments in the Arabian Sea: Implications for the TEX<sub>86</sub>  
901 paleothermometer. *Geochimica et Cosmochimica Acta*, 142, 386–399.  
902 <https://doi.org/10.1016/j.gca.2014.07.013>
- 903 Lengger, S. K., Sutton, P. A., Rowland, S. J., Hurley, S. J., Pearson, A., Naafs, B. D. A., et al.  
904 (2018). Archaeal and bacterial glycerol dialkyl glycerol tetraether (GDGT) lipids in  
905 environmental samples by high temperature-gas chromatography with flame ionization and time-  
906 of-flight mass spectrometry detection. *Organic Geochemistry*, 121, 10–21.  
907 <https://doi.org/10.1016/j.orggeochem.2018.03.012>
- 908 Liu, K.-K., Kao, S.-J., Hu, H.-C., Chou, W.-C., Hung, G.-W., & Tseng, C.-M. (2007). Carbon  
909 isotopic composition of suspended and sinking particulate organic matter in the northern South  
910 China Sea—From production to deposition. *Deep Sea Research Part II: Topical Studies in  
911 Oceanography*, 54(14), 1504–1527. <https://doi.org/10.1016/j.dsr2.2007.05.010>
- 912 Lüke, C., Speth, D. R., Kox, M. A. R., Villanueva, L., & Jetten, M. S. M. (2016). Metagenomic  
913 analysis of nitrogen and methane cycling in the Arabian Sea oxygen minimum zone. *PeerJ*, 4,  
914 e1924. <https://doi.org/10.7717/peerj.1924>
- 915 Luo, G., Algeo, T. J., Huang, J., Zhou, W., Wang, Y., Yang, H., et al. (2014). Vertical δ<sup>13</sup>C<sub>org</sub>  
916 gradients record changes in planktonic microbial community composition during the end-  
917 Permian mass extinction. *Palaeogeography, Palaeoclimatology, Palaeoecology*, 396, 119–131.  
918 <https://doi.org/10.1016/j.palaeo.2014.01.006>
- 919 Matys, E. D., Sepúlveda, J., Pantoja, S., Lange, C. B., Caniupán, M., Lamy, F., & Summons, R.  
920 E. (2017). Bacteriohopanepolyols along redox gradients in the Humboldt Current System off  
921 northern Chile. *Geobiology*, 15(6), 844–857. <https://doi.org/10.1111/gbi.12250>
- 922 Meyers, P. A. (2014). Why are the δ<sup>13</sup>C<sub>org</sub> values in Phanerozoic black shales more negative  
923 than in modern marine organic matter? *Geochemistry, Geophysics, Geosystems*, 15(7), 3085–  
924 3106. <https://doi.org/10.1002/2014GC005305>
- 925 Meyers, P. A., & Arnaboldi, M. (2008). Paleoceanographic implications of nitrogen and organic  
926 carbon isotopic excursions in mid-Pleistocene sapropels from the Tyrrhenian and Levantine  
927 Basins, Mediterranean Sea. *Palaeogeography, Palaeoclimatology, Palaeoecology*, 266(1), 112–  
928 118. <https://doi.org/10.1016/j.palaeo.2008.03.018>
- 929 Middelburg, J. J. (1989). A simple rate model for organic matter decomposition in marine  
930 sediments. *Geochimica et Cosmochimica Acta*, 53(7), 1577–1581. [https://doi.org/10.1016/0016-7037\(89\)90239-1](https://doi.org/10.1016/0016-7037(89)90239-1)

- 932 Middelburg, J. J., Vlug, T., Jaco, F., & van der Nat, W. A. (1993). Organic matter mineralization  
933 in marine systems. *Global and Planetary Change*, 8(1), 47–58. <https://doi.org/10.1016/0921->  
934 8181(93)90062-S
- 935 Middelburg J. J. (2011). Chemoautotrophy in the ocean. *Geophysical Research Letters*, 38(24).  
936 <https://doi.org/10.1029/2011GL049725>
- 937 Moos, C. (2000). *Reconstruction of upwelling intensity and paleo-nutrient gradients in the*  
938 *Northwest Arabian Sea derived from stable carbon and oxygen isotopes of planktic foraminifera*.  
939 University of Bremen, Bremen, Germany. Retrieved from <http://elib.suub.uni-bremen.de/ip/docs/00010276.pdf>
- 941 Naqvi, S. W. A., & Shailaja, M. S. (1993). Activity of the respiratory electron transport system  
942 and respiration rates within the oxygen minimum layer of the Arabian Sea. *Deep Sea Research*  
943 *Part II: Topical Studies in Oceanography*, 40(3), 687–695. <https://doi.org/10.1016/0967->  
944 0645(93)90052-O
- 945 Nierop, K. G. J., Reichart, G.-J., Veld, H., & Sinninghe Damsté, J. S. (2017). The influence of  
946 oxygen exposure time on the composition of macromolecular organic matter as revealed by  
947 surface sediments on the Murray Ridge (Arabian Sea). *Geochimica et Cosmochimica Acta*, 206,  
948 40–56. <https://doi.org/10.1016/j.gca.2017.02.032>
- 949 Pachiadaki, M. G., Sintes, E., Bergauer, K., Brown, J. M., Record, N. R., Swan, B. K., et al.  
950 (2017). Major role of nitrite-oxidizing bacteria in dark ocean carbon fixation. *Science*,  
951 358(6366), 1046–1051. <https://doi.org/10.1126/science.aan8260>
- 952 Pagani, M. (2005). Marked Decline in Atmospheric Carbon Dioxide Concentrations During the  
953 Paleogene. *Science*, 309(5734), 600–603. <https://doi.org/10.1126/science.1110063>
- 954 Pancost, R. D., & Pagani, M. (2005). Controls on the Carbon Isotopic Compositions of Lipids in  
955 Marine Environments. In *Marine Organic Matter: Biomarkers, Isotopes and DNA* (pp. 209–  
956 249). Springer, Berlin, Heidelberg. [https://doi.org/10.1007/698\\_2\\_007](https://doi.org/10.1007/698_2_007)
- 958 Pancost, R. D., & Sinninghe Damsté, J. S. (2003). Carbon isotopic compositions of prokaryotic  
959 lipids as tracers of carbon cycling in diverse settings. *Chemical Geology*, 195(1–4), 29–58.  
960 [https://doi.org/10.1016/S0009-2541\(02\)00387-X](https://doi.org/10.1016/S0009-2541(02)00387-X)
- 961 Pancost, R. D., Freeman, K. H., & Patzkowsky, M. E. (1999). Organic-matter source variation  
962 and the expression of a late Middle Ordovician carbon isotope excursion. *Geology*, 27(11),  
963 1015–1018. [https://doi.org/10.1130/0091-7613\(1999\)027<1015:OMSVAT>2.3.CO;2](https://doi.org/10.1130/0091-7613(1999)027<1015:OMSVAT>2.3.CO;2)
- 964 Pancost, R. D., Steart, D. S., Handley, L., Collinson, M. E., Hooker, J. J., Scott, A. C., et al.  
965 (2007). Increased terrestrial methane cycling at the Palaeocene–Eocene thermal maximum.  
966 *Nature*, 449(7160), 332–335. <https://doi.org/10.1038/nature06012>

- 967 Pancost, R. D., Freeman, K. H., Herrmann, A. D., Patzkowsky, M. E., Ainsaar, L., & Martma, T.  
968 (2013). Reconstructing Late Ordovician carbon cycle variations. *Geochimica et Cosmochimica  
969 Acta*, 105, 433–454. <https://doi.org/10.1016/j.gca.2012.11.033>
- 970 Parnell, A. C., Inger, R., Bearhop, S., & Jackson, A. L. (2010). Source Partitioning Using Stable  
971 Isotopes: Coping with Too Much Variation. *PLOS ONE*, 5(3), e9672.  
972 <https://doi.org/10.1371/journal.pone.0009672>
- 973 Paulmier, A., & Ruiz-Pino, D. (2009). Oxygen minimum zones (OMZs) in the modern ocean.  
974 *Progress in Oceanography*, 80(3–4), 113–128. <https://doi.org/10.1016/j.pocean.2008.08.001>
- 975 Pearson, A. (2010). Pathways of Carbon Assimilation and Their Impact on Organic Matter  
976 Values  $\delta^{13}\text{C}$ . In K. N. Timmis (Ed.), *Handbook of Hydrocarbon and Lipid Microbiology* (pp.  
977 143–156). Berlin, Heidelberg: Springer Berlin Heidelberg. Retrieved from  
978 [http://link.springer.com/10.1007/978-3-540-77587-4\\_9](http://link.springer.com/10.1007/978-3-540-77587-4_9)
- 979 Pearson, Ann, & Rusch, D. B. (2009). Distribution of microbial terpenoid lipid cyclases in the  
980 global ocean metagenome. *The ISME Journal*, 3(3), 352–363.  
981 <https://doi.org/10.1038/ismej.2008.116>
- 982 Phillips, D. L., Newsome, S. D., & Gregg, J. W. (2005). Combining sources in stable isotope  
983 mixing models: alternative methods. *Oecologia*, 144(4), 520–527.  
984 <https://doi.org/10.1007/s00442-004-1816-8>
- 985 Pitcher, A., Villanueva, L., Hopmans, E. C., Schouten, S., Reichart, G.-J., & Sinninghe Damsté,  
986 J. S. (2011). Niche segregation of ammonia-oxidizing archaea and anammox bacteria in the  
987 Arabian Sea oxygen minimum zone. *The ISME Journal*, 5(12), 1896–1904.  
988 <https://doi.org/10.1038/ismej.2011.60>
- 989 Pozzato, L., Oevelen, D. V., Moodley, L., Soetaert, K., & Middelburg, J. J. (2013a). Sink or  
990 link? The bacterial role in benthic carbon cycling in the Arabian Sea's oxygen minimum zone.  
991 *Biogeosciences*, 10(11), 6879–6891. <https://doi.org/10.5194/bg-10-6879-2013>
- 992 Pozzato, Lara, van Oevelen, D., Moodley, L., Soetaert, K., & Middelburg, J. J. (2013b). Carbon  
993 processing at the deep-sea floor of the Arabian Sea oxygen minimum zone: A tracer approach.  
994 *Journal of Sea Research*, 78, 45–58. <https://doi.org/10.1016/j.seares.2013.01.002>
- 995 Queste, B. Y., Vic, C., Heywood, K. J., & Piontkovski, S. A. (2018). Physical Controls on  
996 Oxygen Distribution and Denitrification Potential in the North West Arabian Sea. *Geophysical  
997 Research Letters*, 45(9), 4143–4152. <https://doi.org/10.1029/2017GL076666>
- 998 Reinthaler, T., van Aken, H. M., & Herndl, G. J. (2010). Major contribution of autotrophy to  
999 microbial carbon cycling in the deep North Atlantic's interior. *Deep Sea Research Part II:  
1000 Topical Studies in Oceanography*, 57(16), 1572–1580.  
1001 <https://doi.org/10.1016/j.dsr2.2010.02.023>

- 1002 Rixen, T., & Ittekkot, V. (2005). Nitrogen deficits in the Arabian Sea, implications from a three  
1003 component mixing analysis. *Deep Sea Research Part II: Topical Studies in Oceanography*,  
1004 52(14–15), 1879–1891. <https://doi.org/10.1016/j.dsr2.2005.06.007>
- 1005 Roullier, F., Berline, L., Guidi, L., Durrieu De Madron, X., Picheral, M., Sciandra, A., et al.  
1006 (2014). Particle size distribution and estimated carbon flux across the Arabian Sea oxygen  
1007 minimum zone. *Biogeosciences*, 11(16), 4541–4557. <https://doi.org/10.5194/bg-11-4541-2014>
- 1008 Rush, D., & Sinninghe Damsté, J. S. (2017). Lipids as paleomarkers to constrain the marine  
1009 nitrogen cycle: Lipids as paleomarkers. *Environmental Microbiology*, 19(6), 2119–2132.  
1010 <https://doi.org/10.1111/1462-2920.13682>
- 1011 Rush, D., Sinninghe Damsté, J. S., Poulton, S. W., Thamdrup, B., Garside, A. L., Acuña  
1012 González, J., et al. (2014). Anaerobic ammonium-oxidising bacteria: A biological source of the  
1013 bacteriohopanetetrol stereoisomer in marine sediments. *Geochimica et Cosmochimica Acta*, 140,  
1014 50–64. <https://doi.org/10.1016/j.gca.2014.05.014>
- 1015 Rush, D., Talbot, H. M., Meer, M. T. J. van der, Hopmans, E. C., Douglas, B., & Sinninghe  
1016 Damsté, J. S. (2019). Biomarker evidence for the occurrence of anaerobic ammonium oxidation  
1017 in the eastern Mediterranean Sea during Quaternary and Pliocene sapropel formation.  
1018 *Biogeosciences Discussions*, 1–27. <https://doi.org/10.5194/bg-2019-27>
- 1019 Sáenz, J. P., Wakeham, S. G., Eglinton, T. I., & Summons, R. E. (2011). New constraints on the  
1020 provenance of hopanoids in the marine geologic record: Bacteriohopanepolyols in marine  
1021 suboxic and anoxic environments. *Organic Geochemistry*, 42(11), 1351–1362.  
1022 <https://doi.org/10.1016/j.orggeochem.2011.08.016>
- 1023 Sakata, S., Hayes, J. M., McTaggart, A. R., Evans, R. A., Leckrone, K. J., & Togasaki, R. K.  
1024 (1997). Carbon isotopic fractionation associated with lipid biosynthesis by a cyanobacterium:  
1025 Relevance for interpretation of biomarker records. *Geochimica et Cosmochimica Acta*, 61(24),  
1026 5379–5389. [https://doi.org/10.1016/S0016-7037\(97\)00314-1](https://doi.org/10.1016/S0016-7037(97)00314-1)
- 1027 Schenau, S. J., Passier, H. F., Reichart, G. J., & de Lange, G. J. (2002). Sedimentary pyrite  
1028 formation in the Arabian Sea. *Marine Geology*, 185(3), 393–402. [https://doi.org/10.1016/S0025-3227\(02\)00183-4](https://doi.org/10.1016/S0025-3227(02)00183-4)
- 1030 Schlitzer, R. (2002). Carbon export fluxes in the Southern Ocean: results from inverse modeling  
1031 and comparison with satellite-based estimates. *Deep Sea Research Part II: Topical Studies in  
1032 Oceanography*, 49(9), 1623–1644. [https://doi.org/10.1016/S0967-0645\(02\)00004-8](https://doi.org/10.1016/S0967-0645(02)00004-8)
- 1033 Schmaljohann, R., Drews, M., Walter, S., Linke, P., Rad, U. von, & Imhoff, J. F. (2001).  
1034 Oxygen-minimum zone sediments in the northeastern Arabian Sea off Pakistan: a habitat for the  
1035 bacterium *Thioploca*. *Marine Ecology Progress Series*, 211, 27–42.  
1036 <https://doi.org/10.3354/meps211027>

- 1037 Schmidtko, S., Stramma, L., & Visbeck, M. (2017). Decline in global oceanic oxygen content  
1038 during the past five decades. *Nature*, 542(7641), 335–339. <https://doi.org/10.1038/nature21399>
- 1039 Schouten, S., Strous, M., Kuypers, M. M. M., Rijpstra, W. I. C., Baas, M., Schubert, C. J., et al.  
1040 (2004). Stable Carbon Isotopic Fractionations Associated with Inorganic Carbon Fixation by  
1041 Anaerobic Ammonium-Oxidizing Bacteria. *Applied and Environmental Microbiology*, 70(6),  
1042 3785–3788. <https://doi.org/10.1128/AEM.70.6.3785-3788.2004>
- 1043 Schouten, Stefan, Klein Breteler, W. C. M., Blokker, P., Schogt, N., Rijpstra, W. I. C., Grice, K.,  
1044 et al. (1998). Biosynthetic effects on the stable carbon isotopic compositions of algal lipids:  
1045 implications for deciphering the carbon isotopic biomarker record. *Geochimica et Cosmochimica  
1046 Acta*, 62(8), 1397–1406. [https://doi.org/10.1016/S0016-7037\(98\)00076-3](https://doi.org/10.1016/S0016-7037(98)00076-3)
- 1047 Schouten, Stefan, Hoefs, M. J. L., & Sinninghe Damsté, J. S. (2000). A molecular and stable  
1048 carbon isotopic study of lipids in late Quaternary sediments from the Arabian Sea. *Organic  
1049 Geochemistry*, 31(6), 509–521. [https://doi.org/10.1016/S0146-6380\(00\)00031-0](https://doi.org/10.1016/S0146-6380(00)00031-0)
- 1050 Schouten, Stefan, Pitcher, A., Hopmans, E. C., Villanueva, L., van Bleijswijk, J., & Sinninghe  
1051 Damsté, J. S. (2012). Intact polar and core glycerol dibiphytanyl glycerol tetraether lipids in the  
1052 Arabian Sea oxygen minimum zone: I. Selective preservation and degradation in the water  
1053 column and consequences for the TEX86. *Geochimica et Cosmochimica Acta*, 98, 228–243.  
1054 <https://doi.org/10.1016/j.gca.2012.05.002>
- 1055 Sessions, A. L., Zhang, L., Welander, P. V., Doughty, D., Summons, R. E., & Newman, D. K.  
1056 (2013). Identification and quantification of polyfunctionalized hopanoids by high temperature  
1057 gas chromatography–mass spectrometry. *Organic Geochemistry*, 56, 120–130.  
1058 <https://doi.org/10.1016/j.orggeochem.2012.12.009>
- 1059 Shaffer, G., Olsen, S. M., & Pedersen, J. O. P. (2009). Long-term ocean oxygen depletion in  
1060 response to carbon dioxide emissions from fossil fuels. *Nature Geoscience*, 2(2), 105–109.  
1061 <https://doi.org/10.1038/ngeo420>
- 1062 Sokoll, S., Holtappels, M., Lam, P., Collins, G., Schlüter, M., Lavik, G., & Kuypers, M. M. M.  
1063 (2012). Benthic Nitrogen Loss in the Arabian Sea Off Pakistan. *Frontiers in Microbiology*, 3.  
1064 <https://doi.org/10.3389/fmicb.2012.00395>
- 1065 Spiker, E. C., & Hatcher, P. G. (1987). The effects of early diagenesis on the chemical and stable  
1066 carbon isotopic composition of wood. *Geochimica et Cosmochimica Acta*, 51(6), 1385–1391.  
1067 [https://doi.org/10.1016/0016-7037\(87\)90323-1](https://doi.org/10.1016/0016-7037(87)90323-1)
- 1068 Stramma, L., Schmidtko, S., Levin, L. A., & Johnson, G. C. (2010). Ocean oxygen minima  
1069 expansions and their biological impacts. *Deep Sea Research Part I: Oceanographic Research  
1070 Papers*, 57(4), 587–595. <https://doi.org/10.1016/j.dsr.2010.01.005>
- 1071 Strous, M., Kuenen, J. G., & Jetten, M. S. M. (1999). Key Physiology of Anaerobic Ammonium  
1072 Oxidation. *Applied and Environmental Microbiology*, 65(7), 3248–3250.

- 1073 Talbot, H. M., Rohmer, M., & Farrimond, P. (2007). Rapid structural elucidation of composite  
1074 bacterial hopanoids by atmospheric pressure chemical ionization liquid chromatography/ion trap  
1075 mass spectrometry. *Rapid Communications in Mass Spectrometry*, 21(6), 880–892.  
1076 <https://doi.org/10.1002/rcm.2911>
- 1077 Taylor, G. T., Iabichella, M., Ho, T.-Y., Scranton, M. I., Thunell, R. C., Muller-Karger, F., &  
1078 Varela, R. (2001). Chemoautotrophy in the redox transition zone of the Cariaco Basin: A  
1079 significant midwater source of organic carbon production. *Limnology and Oceanography*, 46(1),  
1080 148–163. <https://doi.org/10.4319/lo.2001.46.1.0148>
- 1081 Ulloa, O., Canfield, D. E., DeLong, E. F., Letelier, R. M., & Stewart, F. J. (2012). Microbial  
1082 oceanography of anoxic oxygen minimum zones. *Proceedings of the National Academy of  
1083 Sciences of the United States of America*, 109(40), 15996–16003.  
1084 <https://doi.org/10.1073/pnas.1205009109>
- 1085 Van Kaam-Peters, H. M. E., Schouten, S., Köster, J., & Sinninghe Damstè, J. S. (1998). Controls  
1086 on the molecular and carbon isotopic composition of organic matter deposited in a  
1087 Kimmeridgian euxinic shelf sea: evidence for preservation of carbohydrates through  
1088 sulfurization. *Geochimica et Cosmochimica Acta*, 62(19), 3259–3283.  
1089 [https://doi.org/10.1016/S0016-7037\(98\)00231-2](https://doi.org/10.1016/S0016-7037(98)00231-2)
- 1090 Villanueva, L., Speth, D. R., Vanalen, T., Hoischen, A., & Jetten, M. (2014). Shotgun  
1091 metagenomic data reveals significant abundance but low diversity of “Candidatus Scalindua”  
1092 marine anammox bacteria in the Arabian Sea oxygen minimum zone. *Frontiers in Microbiology*,  
1093 5. <https://doi.org/10.3389/fmicb.2014.00031>
- 1094 van de Vossenberg, J., Rattray, J. E., Geerts, W., Kartal, B., Niftrik, L. V., Donselaar, E. G. V.,  
1095 et al. (2008). Enrichment and characterization of marine anammox bacteria associated with  
1096 global nitrogen gas production. *Environmental Microbiology*, 10(11), 3120–3129.  
1097 <https://doi.org/10.1111/j.1462-2920.2008.01643.x>
- 1098 van de Vossenberg, J., Woebken, D., Maalcke, W. J., Wessels, H. J. C. T., Dutilh, B. E., Kartal,  
1099 B., et al. (2013). The metagenome of the marine anammox bacterium ‘Candidatus Scalindua  
1100 profunda’ illustrates the versatility of this globally important nitrogen cycle bacterium.  
1101 *Environmental Microbiology*, 15(5), 1275–1289. [https://doi.org/10.1111/j.1462-2920.2012.02774.x](https://doi.org/10.1111/j.1462-<br/>1102 2920.2012.02774.x)
- 1103 Wakeham, S. G., & McNichol, A. P. (2014). Transfer of organic carbon through marine water  
1104 columns to sediments – insights from stable and radiocarbon isotopes of lipid biomarkers.  
1105 *Biogeosciences*, 11(23), 6895–6914. <https://doi.org/10.5194/bg-11-6895-2014>
- 1106 Wakeham, Stuart G., Peterson, M. L., Hedges, J. I., & Lee, C. (2002). Lipid biomarker fluxes in  
1107 the Arabian Sea, with a comparison to the equatorial Pacific Ocean. *Deep Sea Research Part II:  
1108 Topical Studies in Oceanography*, 49(12), 2265–2301. [https://doi.org/10.1016/S0967-0645\(02\)00037-1](https://doi.org/10.1016/S0967-<br/>1109 0645(02)00037-1)

- 1110 Ward, B. B., Devol, A. H., Rich, J. J., Chang, B. X., Bulow, S. E., Naik, H., et al. (2009).  
1111 Denitrification as the dominant nitrogen loss process in the Arabian Sea. *Nature*, 461(7260), 78–  
1112 81. <https://doi.org/10.1038/nature08276>
- 1113 van Winden, J. F., Talbot, H. M., Kip, N., Reichart, G.-J., Pol, A., McNamara, N. P., et al.  
1114 (2012). Bacteriohopanepolyol signatures as markers for methanotrophic bacteria in peat moss.  
1115 *Geochimica et Cosmochimica Acta*, 77, 52–61. <https://doi.org/10.1016/j.gca.2011.10.026>
- 1116 Witkowski, C. R., Weijers, J. W. H., Blais, B., Schouten, S., & Damsté, J. S. S. (2018).  
1117 Molecular fossils from phytoplankton reveal secular pCO<sub>2</sub> trend over the Phanerozoic. *Science  
1118 Advances*, 4(11), eaat4556. <https://doi.org/10.1126/sciadv.aat4556>
- 1119 Wright, J. J., Konwar, K. M., & Hallam, S. J. (2012). Microbial ecology of expanding oxygen  
1120 minimum zones. *Nature Reviews Microbiology*, 10(6), 381–394.  
1121 <https://doi.org/10.1038/nrmicro2778>
- 1122 Wuchter, C. (2006). Archaeal nitrification in the ocean. *Proceedings of the National Academy of  
1123 Sciences*, 103(33), 12317–12322. <https://doi.org/10.1073/pnas.0600756103>
- 1124 Zachos, J. C., Röhl, U., Schellenberg, S. A., Sluijs, A., Hodell, D. A., Kelly, D. C., et al. (2005).  
1125 Rapid Acidification of the Ocean During the Paleocene-Eocene Thermal Maximum. *Science*,  
1126 308(5728), 1611–1615. <https://doi.org/10.1126/science.1109004>
- 1127 Zhang, C. L., Huang, Z., Cantu, J., Pancost, R. D., Brigmon, R. L., Lyons, T. W., & Sassen, R.  
1128 (2005). Lipid Biomarkers and Carbon Isotope Signatures of a Microbial (Beggiatoa) Mat  
1129 Associated with Gas Hydrates in the Gulf of Mexico. *Applied and Environmental Microbiology*,  
1130 71(4), 2106–2112. <https://doi.org/10.1128/AEM.71.4.2106-2112.2005>
- 1131 Ziegler, M., Jilbert, T., de Lange, G. J., Lourens, L. J., & Reichart, G.-J. (2008). Bromine counts  
1132 from XRF scanning as an estimate of the marine organic carbon content of sediment cores:  
1133 Bromine as estimator for sediment composition. *Geochemistry, Geophysics, Geosystems*, 9(5).  
1134 <https://doi.org/10.1029/2007GC001932>
- 1135  
1136  
1137  
1138  
1139  
1140  
1141  
1142  
1143  
1144  
1145

1146

1147 **Table 1.**  $\delta^{13}\text{C}$  values of analysed samples. s.d. = standard deviation of three repeat analyses, n.d.  
1148 = not determined (single analysis). The values shown are natural abundance from unamended  
1149 cores, and from incubations with  $^{13}\text{C}$  labelled DOM and POM, under oxic and suboxic  
1150 conditions. \* indicates outliers (Grubbs).

<b>Type</b>	<b>Sample</b>	<b><math>\delta^{13}\text{C}</math> value [‰ V-PDB]</b>			
		<b>BHT</b>	<b>s.d.</b>	<b>BHT'</b>	<b>s.d.</b>
Biomass	Scalindua sp.	-47.8	1	-47.6	1
	P900 - 1 cm	-24.7	1.3	-39.1	1.3
Arabian Sea	P900 - 3 cm	-27.0	1.4	-48.1	1.1
Natural abundance	P900 - 7 cm	-26.1	0.4	-41.4	0.5
	P1800 - 1 cm	-25.1	1.7	-48.1	1.6
	P1800 - 3 cm	-28.8	2.1	-46.6	4.1
	P1800 - 7 cm	-27.1	0.6	-45.5	1.0
	P900, suboxic, DOM - 1 cm	-27.9	n.d.	-45.9	n.d.
	P900, suboxic, DOM - 3 cm	-26.6	n.d.	-42.0	n.d.
	P900, suboxic, POM - 1 cm	-41.6*	n.d.	-75.2*	n.d.
	P900, suboxic, POM - 3 cm	-26.4	n.d.	-49.8	n.d.
Arabian Sea	P900, oxic, POM - 1 cm	-27.1	n.d.	-51.5	n.d.
Incubations	P900, oxic, POM - 3 cm	-25.2	n.d.	-47.8	n.d.
	P1800, oxic, DOM - 1 cm	-21.3	n.d.	-42.0	n.d.
	P1800, oxic, DOM - 3 cm	-28.3	n.d.	-45.6	n.d.
	P1800, suboxic, POM - 1 cm	-52.2*	n.d.	-101.9*	n.d.
	P1800, suboxic, POM - 3 cm	-28.8	n.d.	-47.1	n.d.
	P1800, oxic, POM - 1 cm	-30.2	n.d.	-51.3	n.d.
	P1800, oxic, POM - 3 cm	-28.0	n.d.	-46.1	n.d.

1151